Quasielastic knockout of clusters by fast protons at large momentum transfers and nuclear structure

M. A. Zhusupov and Yu. N. Uzikov

Kazakh State University, Alma-Ata

Fiz. Elem. Chastits At. Yadra **18**, 323–373 (March–April 1987)

Present ideas about nucleon clustering in nuclei are reviewed. The main attention is devoted to the role of excited clusters in the ground states of $1p$-shell nuclei. Their properties, their status outside the framework of the translationally invariant shell model, and the conditions most favorable for manifestation of their contribution to nuclear reaction cross sections are discussed. It is shown that in (p, Nx) quasielastic knockout reactions the contribution of excited clusters, x^*, may be the most important at large momentum transfer. The results are given of calculation of the characteristics of quasielastic knockout of d, t, and α particles at energies around 0.7 GeV at momentum transfer 5–10 F^{-1} with allowance for processes that take place on excited clusters, $px^* \to Nx$, which are treated on the basis of existing ideas about the mechanisms of proton backward elastic scattering by the lightest nuclei in the corresponding range of energies.

INTRODUCTION

In this review, we consider reactions involving the quasielastic knockout of nucleon clusters (QKNC) induced by protons at energies of several hundred mega-electronvolts. The quasielastic knockout process $p + A \to p + x + B$, where x is the cluster that is knocked out, A is the initial nucleus, and B is the residual nucleus, has kinematics in the laboratory frame very similar to the kinematics of proton elastic scattering by a free cluster at rest: $p + x \to p + x$. Because of this striking kinematic feature, QKNC reactions are usually regarded as direct proof of the existence of clusters in nuclei and are widely used to study the cluster structure of nuclei.[1] By means of QKNC reactions of the type (p,pd), (p, pt), $(p, p\alpha)$, $(\alpha, 2\alpha)$ extensive spectroscopic information has been accumulated about the momentum distributions of clusters in nuclei and their effective numbers.[2]

The QKNC reactions at high energies under conditions of a large momentum transfer are particularly interesting, since in this case the characteristics of the process may contain information about the short-range NN correlations in nuclei. It is sufficient to recall in this connection that the first attempt to understand the inclusive Dubna data[3] on quasielastic knockout of fast deuterons generated the hypothesis of fluctuations of the nuclear matter density.[4] Subsequently, this idea, enriched by ideas about the quark structure of hadrons, became one of the points of departure in the prediction and study of the cumulative effect.[5] The discovery of the quark structure of the nucleon and the possibility associated with it of the existence of multiquark configurations in nuclei may be important for QKNC reactions at large momentum transfers. However, the connection between QKNC reactions and the quark degrees of freedom in nuclei requires further investigation. In contrast to this direction, the development of systematic theoretical ideas about QKNC reactions took place in the framework of ordinary ideas about nuclear structure.[6] The basic principles of a microscopic theory were formulated; the main feature of this theory is the principle of fractional parentage of nuclear states.[7] It was established that the spectroscopic information extracted from QKNC reactions fits in well with widely accepted shell ideas about nuclear structure.[8,9] An analysis of the experimental and theoretical situation with regard to QKNC reactions at large momentum transfers at the middle of the seventies can be found in Ref. 10.

During the last decade, definite progress has been achieved in the investigations of QKNC reactions at large momentum transfer. First, besides the "single-arm" data,[3,11] the results of kinematically complete (p, pd) and (p, nd) coincidence experiments have been published.[12,13] Second, new data have been obtained on elastic pd (Ref. 14), p^3He (Ref. 15), and p^4He (Ref. 16) backward scattering at energies around 1 GeV, and the ideas about the mechanisms of these processes have been made more precise; this is of fundamental importance for understanding the dynamics of quasielastic knockout of fast clusters. Third, and, in our view, most important, there has occurred in the theory a deep rethinking of cluster phenomena in QKNC reactions at high energies.[17] We shall dwell on this in more detail.

The usual and widely accepted interpretation of QKNC reactions is as follows.[8] It is assumed that a cluster knocked out of a nucleus existed in the nucleus already before the time of interaction and that its internal state was not changed by the knockout process. As a rule, this approximation works well in the region of intermediate energies, up to about 100–150 MeV, where, because of the strong absorption, the QKNC reactions have a clearly peripheral nature. However, a treatment of the reaction as simplified as this may not be viable at energies around 1 GeV; for as the initial energy is increased from 0.1 to 1 GeV the contribution of the interior region of the nucleus to the QKNC cross section increases appreciably (see, for example, Fig. 1 for the $(\alpha, 2\alpha)$ reaction from Ref. 19), and in this region, in contrast to the peripheral region, modern ideas about nuclear structure indicate that the dominant components of the nuclear wave function do not contain ordinary d, t, and α clusters.[20] Therefore, in the theory of QKNC reactions at high energies it becomes an important task to find the probability of the following process: An incident proton (hadron) interacts with a group of nucleons of the nucleus that in the general case is not a d, t, or α cluster, differs from it in its quantum numbers, and is

 0090-4759/87/020136-23$04.40

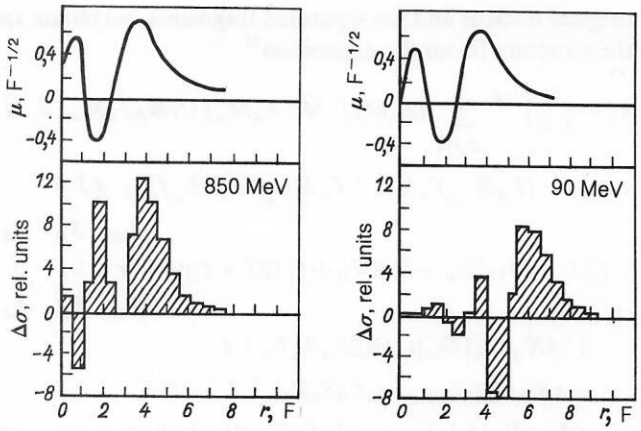

FIG. 1. Radial localization of the $^{16}O(\alpha, 2\alpha)^{12}C$ reaction according to the results of Ref. 19: $u(r)$ is the wave function of the 3S state in the $^{16}O \to \alpha + {}^{12}C$ channel; $\Delta\sigma$ is the histogram of the contributions to the $^{16}O(\alpha, 2\alpha)^{12}C$ reaction cross section as a function of the distance from the center of the nucleus for recoil momentum $k_B = 0$.

called in what follows an excited cluster (a more accurate definition is given below), but in the process of interaction an ordinary cluster is formed from this group and is then observed in the final state. This problem can be formulated mathematically in the framework of the translationally invariant shell model (TISM).

Indeed, in the fractional-parentage expansion of the TISM wave function for the ground state of nucleus A in the channel $A \to x + B$ one can separate two terms:

$$\psi_A = C\psi_x\psi_B\psi_\gamma(\rho_{xB}) + \sum_{x^*B^*\gamma^*} C'\psi_{x^*}\psi_{B^*}\psi_{\gamma^*}(\rho_{xB}). \qquad (1)$$

The first term contains the ordinary cluster x and the residual nucleus B in their ground states ψ_x and ψ_B with respect to the internal motion, which are coupled by the function $\psi_\gamma(\rho_{xB})$ of the relative motion.

In the second term, the cluster x^* (respectively, the nucleus B^*) is the same as the cluster x (respectively, B) only as regards the number of nucleons, differing from it in the quantum numbers of the internal motion, and the corresponding function of the mutual motion of the centers of mass of x^* and B^*, $\psi_{\gamma^*}(\rho_{xB})$, is drawn into the nucleus. The basis of the approach to QKNC reactions developed by Neudatchin *et al.*[21] for small initial angles of the secondary protons is based on combination of the TISM with Glauber–Sitenko multiple-scattering theory. The constructive nature of this "dynamical" approach, due to the reliability of the wave functions and the mechanism of the elementary interaction, made it possible to predict a number of interesting results completely absent in the traditional treatment of QKNC reactions and amenable to experimental verification. In the region of large momentum transfers, corresponding to emission of protons in the backward hemisphere, the analogous problem encounters great difficulties, since neither the interaction mechanisms nor the large-momentum components of the nuclear wave functions are sufficiently well known. Nevertheless, in this case too some results have been obtained, qualitative rather than quantitative. In the present review, our main attention is devoted to this problem.

1. TRANSLATIONALLY INVARIANT SHELL MODEL AND EXCITED NUCLEON CLUSTERS IN NUCLEI

In the region of light nuclei with $A \leqslant 16$ the structure factors of the d, t, and α particles can be calculated by a method developed in detail in the framework of the shell model and based on the principles of fractional parentage of nuclear states.[1,22] Since its creation (1950–1960), this method has been subjected to wide experimental testing. It has been established that in the majority of cases the d, t, and α spectroscopic factors extracted at low and intermediate energies from different reactions (quasielastic knockout, many-nucleon transfer) not only agree fully with each other but also fit well with shell ideas about nuclear structure. There is no doubt that this result is a great achievement in the theory of cluster phenomena in nuclei. It should, however, be emphasized that so far it is the spectroscopic factors for clusters in the ground states of their internal motion that have, as a rule, been compared with experiment, and it is transitions to levels of the residual nuclei with unbroken internal shells that are discussed.[8,9] In other words, in the experimental testing of the fractional-parentage conception only the first term in the expansion (1) is taken into account, and all the remaining terms are effectively ignored. At the present time, the problem of taking into account these terms has in principle been solved, and the most complete exposition of this work can be found in Ref. 23. Allowance for the second term in the expansion (1) leads to the representation of excited clusters in the ground states of the nuclei and requires an appropriate generalization of the concept of a spectroscopic factor. What is the weight of these terms in the nuclear wave function? Why are they not manifested in the known experimental data, and under what conditions can they be discovered in an experiment? What is the status of the excited clusters outside the framework of the shell model? This and the following sections are devoted to a qualitative consideration of these questions.

Definitions

The structure factor for separation from a nucleus with mass number A of an excited cluster x is defined in the same way as for an unexcited cluster, by an overlap integral[23]:

$$S_A^x = \binom{A}{x}^{1/2} \langle \psi_A \mid \psi_B\psi_{\nu\Lambda}(\mathbf{R}_{A-x} - \mathbf{R}_x)\,\psi_x \rangle, \qquad (2)$$

where the functions ψ_A, ψ_B, ψ_x, which are antisymmetrized with respect to all nucleons, describe the internal motion in the initial nucleus A, in the residual nucleus $A - x$, and in the distinguished cluster x, respectively; $\psi_{\nu\Lambda}(\mathbf{R}_{A-x} - \mathbf{R}_x)$ is the wave function of the relative motion of the centers of mass of the separated fragments $A - x$ and x in a bound state; ν and Λ are the principal quantum number (the number of oscillator quanta) and the orbital angular momentum of the relative motion; and the binomial factor $(A/x) = A!/x!(A-x)!$ takes into account the identity of the nucleons. For the description of the decay of the nucleus into two strongly excited fragments (with broken internal shells) in the ordinary shell model the problem arises of eliminating the admixture of spurious states due to unphysical oscillations of the centers of mass of these fragments. To avoid this difficulty but to preserve the possibility of using the Racah-algebra formalism and the technique of fractional-parentage coefficients, it is necessary to use the TISM.[1] In it, the internal state of a nucleus of A nucleons corresponding to definite values of the orbital, L, spin, S, and total, J, angular momenta, and also the isospin T, is described by an antisymmetrized oscillator function

$$\psi_A^{\text{TISM}} = |\, AN\,[f]\,(\lambda\mu)\,\alpha LSTJMM_T\rangle, \qquad (3)$$

where N is the number of oscillator quanta; $[f]$ is the Young diagram that determines the symmetry of the orbital part of the wave function with respect to permutation of the nucleons; $(\lambda\mu)$ is the Elliott symbol that characterizes the symmetry of the state with respect to permutation of the oscillator quanta [SU(3) symmetry of the state]; M and M_T are the projections of the total angular momentum and the isospin; and α represents all the additional quantum numbers needed for unique description of the state. To describe low-lying excited states of nuclei with $A \leqslant 16$ corresponding to the configuration s^4p^{A-4}, one uses the intermediate-coupling model on the basis of the TISM:

$$\psi^A_{J,T} = \sum_{[f]LS} \alpha^{A,JT}_{[f]LS}\, |\, AN\,[f]\,(\lambda\mu)\,\alpha LSTJMM_T\rangle. \qquad (4)$$

The coefficients α in (4) are determined by diagonalizing the shell Hamiltonian, which includes an average field and spin–orbit and residual pairing interactions. For nuclei with $4 \leqslant A \leqslant 16$, the coefficients α have been tabulated.[24] In the frequently employed limit of LS coupling, the expansion (4) contains only one term.

To calculate the integral (2) in the TISM, it is sufficient to know the fractional-parentage expansion of the wave function of nucleus A with respect to the product of TISM functions of the cluster x, the residual nucleus $A - x \equiv B$, and the function of their relative motion:

$$|\, AN_A\alpha\rangle = \sum_{\substack{\beta\gamma\Lambda M_\Lambda \\ N_B N_x \nu}} \langle AN_A\alpha \,|\, A - xN_B\beta,\ \nu\Lambda M_\Lambda,\ xN_x\gamma\rangle \times |\, BN_B\beta\rangle\, |\, xN_x\gamma\rangle\, |\, \nu\Lambda M_\Lambda\rangle. \qquad (5)$$

Here, to simplify the expression, we have indicated explicitly only the number of oscillator quanta from the complete set of TISM quantum numbers. The summation over N_B, N_x, and ν is carried out with allowance for the oscillator rule

$$N_A - N_B = N_x + \nu, \qquad (6)$$

which expresses the condition of conservation of the number of excitation quanta. The concept of an excited cluster used here can be most precisely defined on the basis of the expansion (5). Namely, the state $|xN_x\gamma\rangle$ in the expansion (5) of the ground-state wave function of the nucleus is called an excited cluster if the corresponding number of internal excitation quanta N_x satisfies the condition $N_x > N_x^{\min}$. Here, $N_x^{\min}$ is the minimal number of oscillator quanta compatible with the Pauli principle for the given number of nucleons x. For $1p$-shell nuclei, the TISM function for $N = N^{\min}$ is proportional to the $s^4pN^{\min}$ function of the ordinary shell model. If the number of nucleons is $x \leqslant 4$, then we have $N^{\min} = 0$. Finally, a cluster is said to be unexcited, or ordinary, if $N_x = N_x^{\min}$ and all the remaining TISM quantum numbers are equal to the quantum numbers of the principal component of the wave function of the corresponding d, t, or α particle.[1)] Thus, in the TISM the complete expansion of the function (5) includes both ordinary and excited clusters.

Results of calculations of structure factors

Substituting functions of the form (3) in (2) and ignoring the difference between the oscillator parameters for the original nucleus and the separated fragments, we obtain for the structure factor the expression[23]

$$S_A^x = \binom{A}{x}^{1/2} \sum_{\mathscr{L}\bar{J}\bar{M}} (J_B M_B \bar{J}\,\bar{M} \,|\, J_A M_A)\,(\Lambda M_\Lambda J_x M_x \,|\, \bar{J}\,\bar{M}) \times (T_B M_{T_B} T_x M_{T_x} \,|\, T_A M_{T_A})\, U(\Lambda L_x \bar{J}\bar{S}_x;\ \mathscr{L} J_x) \times [(2L_A+1)(2S_A+1)(2J_B+1)(2\bar{J}+1)]^{1/2} \begin{Bmatrix} L_B & S_B & J_B \\ \mathscr{L} & S_x & \bar{J} \\ L_A & S_A & J_A \end{Bmatrix} \times \langle AN_A\,[f_A]\,(\lambda_A\mu_A)\,\alpha_A L_A S_A T_A \,|\, A - xN_B\,[f_B]\,(\lambda_B\mu_B)\,\alpha_B L_B S_B T_B;\ \nu\Lambda,\ xN_x\,[f_x]\,(\lambda_x\mu_x)\,\alpha_x L_x S_x T_x\,(\mathscr{L}):\ L_A S_A T_A\rangle. \qquad (7)$$

The spectroscopic factor is determined by the square of the expression (7). This expression contains the coefficients of fractional parentage of the TISM, Clebsch–Gordan coefficients, Racah coefficients, and $9j$ symbols. A convenient method for calculating the coefficients of fractional parentage of the TISM for sp states based on the connection between the TISM and the ordinary shell model, for which there are extensive tables of coefficients of fractional parentage, was proposed in Ref. 23 (see also Ref. 25). Actual calculations of the structure factors for the separation of excited three- and four-nucleon clusters with the Young diagrams [3], [21] and [4], [31], respectively, from the ^{12}C nucleus in intermediate coupling have been made on the basis of this method in Ref. 26. Transitions to all possible levels of the residual nuclei, including states with a broken s shell in LS coupling, were considered. The structure factors for separation of two-nucleon clusters from the ^{12}C nucleus were calculated in Ref. 27. An application of the method of Ref. 23 for the separation of two and more excited clusters from a $1p$-shell nucleus is given in Ref. 28. The results of these and similar calculations[29] show that the structure factors for excited clusters are comparable to the corresponding values for ordinary clusters. In this connection, the following question arises: Why do the known experimental data on QKNC reactions at energies $T \sim 100$–150 MeV and many-nucleon transfer contain no indications of an appreciable contribution of excited clusters? To answer this question, we consider first the properties of excited clusters.

Properties of excited clusters

An important difference of excited clusters x^* from unexcited clusters x is related to the properties of the wave function $\psi_{\nu\Lambda}(\mathbf{R}_{A-x} - \mathbf{R}_x)$ of the center-of-mass relative motion of the cluster and residual nucleus. If the state of the residual nucleus B is fixed (in particular, $N_B = \text{const}$), then the larger the number N_x of quanta associated with the internal motion of the cluster, the smaller is the number of the quanta ν, in accordance with (6), and the deeper the wave function $\psi_{\nu\Lambda}(\rho = \mathbf{R}_{A-x} - \mathbf{R}_x)$ penetrates into the nucleus. This property of the TISM wave function $\psi_{\nu\Lambda}(\rho)$ reflects the obvious fact that the binding energy in the channel $A \to B + x^*$ is greater than in the channel $A \to B + x$ by the excitation energy of the cluster x^*. For this reason, excited clusters evidently cannot play an important part in the nuclear reactions that are clearly of a peripheral type.

We note here that the oscillator rule (6) in the case of

ordinary clusters ($N_x = 0$) is widely used as a prescription for finding the number of nodes of the relative-motion wave function of a cluster x and the residual nucleus B in a bound state if the xB interaction is described by a (nonoscillator) potential of, for example, Woods–Saxon type.[9,30] The parameters of this potential are fitted to the low-energy characteristics of the bound state $A \equiv x + B$ and xB scattering with the depth of the potential chosen sufficiently great to ensure that all levels with principal quantum number ν from 0 to $\nu = N_A - N_B$ inclusive fit in the discrete spectrum. Then all levels with $\nu < N_A - N_B$ are disregarded, since in the unexcited-cluster–unexcited-residual-nucleus channel they correspond to the shell configurations s^5p^{A-5}, s^6p^{A-6}, etc., which vanish on antisymmetrization. However, interpreting the oscillator rule (6) in a wider sense, i.e., allowing $N_x \neq 0$, we find that these forbidden (for unexcited clusters) states of the center-of-mass motion with $\nu = 0, 1, \ldots, N_A - N_B - 1$ are in fact allowed for excited clusters with the number of quanta $N_x = N_A - N_B, N_A - N_B - 1, \ldots, 1$, respectively.[2)]

In discussing the properties of the wave function $\psi_{\nu\Lambda}(\rho)$, we must also emphasize that the expansion (5) is symmetric with respect to the light cluster x and the heavy residual nucleus B. Namely, components with heavy excited "clusters" $B(N_B > N_B^{\min})$ are present in the expansion of the ground-state wave function of nucleus A on an equal footing with the light excited clusters $x^*(N_x > N_x^{\min})$. It follows from this that if we wish to establish the actual existence of excited clusters in the original nucleus, we are not necessarily restricted to seeking only processes with rearrangement of the light clusters, $x^* \to x$. For this purpose, we could in principle restrict ourselves to observing the excitation spectra of the residual nuclei B produced in direct nuclear reactions as spectators, provided LS coupling is a good approximation for the corresponding hole states of nucleus B. Despite the significant differences between the properties of the fragments x and B, it is here an important circumstance that in the channels $A \to B^*(N_B^{\min} + N^*) + x(N_x^{\min})$ and $A \to B(N_B^{\min}) + x^*(N^* + N_x^{\min})$ with equal numbers N^* of excess internal excitation quanta in x^* and B^* the relative-motion function $\psi_{\nu\Lambda}(\rho)$ of the fragments is the same with the number of oscillator quanta equal to $\nu = N_A - N_B^{\min} - N_x^{\min} - N^*$.

We now consider the properties of the internal states of the excited clusters. For this, we expand the TISM function of a cluster with respect to the functions of the ordinary shell model, $|sp(2s\text{–}2d)\ldots\rangle$, assuming $x \leqslant 4$:

$$|xN_x[f_x]L_x\alpha\rangle = \psi_{000}^{-1}(\mathbf{R}_x)\{\Omega_x|s^{x-N_x}p^{N_x}:[f_x]L_x\alpha\rangle + W_x|s^{x-N_x+1}p^{N_x-2}(2s-2d)^1[f_x]L_x\alpha\rangle \ldots + C_x(N_x)|s^{x-1}(N_xL_x)^1[f_x]\alpha\rangle\}. \quad (8)$$

For an unexcited cluster, we have similarly

$$|xN_x = 0[f_x] = [x]L_x = 0S_xT_x\rangle = \psi_{000}^{-1}(\mathbf{R}_x)|s^x[x]L_x = 0S_xT_x\rangle. \quad (9)$$

In the expansions (8) and (9), $\psi_{000}(\mathbf{R}_x)$ is the ground-state wave function of the cluster center of mass. As can be seen from these expansions, the main and most interesting difference of an excited cluster from an unexcited one is that its internal state contains higher shell configurations. Thus, on separation from a lp-shell nucleus of a cluster with $x = 4$ nucleons the maximal number of excitation quanta of the cluster is $N_x = 4$. All four quanta can be transferred to a single nucleon, to which the final term in (8) corresponds. This means that in such a configuration the high-momentum single-nucleon component is effectively enhanced compared with its average shell value. At the same time, the center of inertia of the cluster is predominantly at rest in the center of mass of the original nucleus A, since Eq. (6) gives us $\nu = 0$. For a lp-shell nucleus in the average shell configuration, in which the momentum of one nucleon is balanced by the total momentum of all the remaining $A - 1$ nucleons of the nucleus (Fig. 2a), the wave function of the nucleon in the momentum representation is $\psi_{11}(p/p_0)$. At the same time, in the maximally excited ($N_x = 4$) four-nucleon cluster whose center of mass is at rest in the nucleus the momentum of one nucleon is balanced by the momenta of the three remaining nucleons (Fig. 2b), and the corresponding momentum distribution has the form $\psi_{4L}(p/\tilde{p}_0)$. The rms momentum of a nucleon in the second case is approximately twice that in the first. Thus, knowledge of the coefficient $C_x(N_x)$ in front of the last term in (8) is very important. A method for calculating these coefficients and also the values of the coefficients of fractional parentage for the separation of one nucleon from excited three- and four-nucleon clusters are given in Ref. 29.

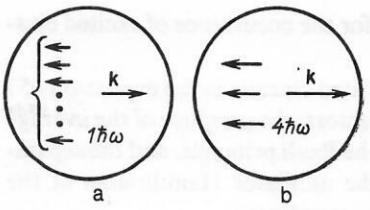

FIG. 2. Momentum distribution of nucleons in the center-of-mass system of a lp-shell nucleus: (a) in the average shell configuration (the momentum of one nucleon is balanced by the total momentum of all the remaining $A - 1$ nucleons), $\psi_{11}(p/p_0)$; (b) in an excited $\langle 4N \rangle$ cluster, $\psi_{4L}(p/\tilde{p}_0)$.

In the case of two-nucleon $\langle 2N \rangle$ clusters, the isospin excitations and radial excitations are not connected and the spatial parts of the wave function for singlet and triplet $\langle 2N \rangle$ clusters in the TISM are the same. This is not so for $\langle 3N \rangle$ and $\langle 4N \rangle$ clusters. In this case, the isospin excitations of a cluster are necessarily accompanied by radial excitations by virtue of the antisymmetrization of the cluster wave function. Thus, the state with $x = 4$ and $T_x = 1$ is not compatible with the spin–isospin Young diagram $[f_{ST}] = [4]$, but the "nonsymmetric" Young diagrams $[f_{ST}]$ equal to [31], [22], [211] are allowed. However, in accordance with the Pauli principle ($[f_{ST}] \circ [f_x] = [1^x]$) the lowest shell configuration $|s^4[f_x] = [4]\rangle$ is not compatible with any of these allowed spin–isospin Young diagrams. Therefore, a $\langle 4N \rangle$ cluster with isospin $T_x = 1$ is necessarily radially excited with $N_x > 0$.

Status of excited clusters outside the framework of the TISM

The TISM describes well a large body of experimental data associated with the first term of the expansion (1). For this reason alone, all the predictions of the model that follow from the second term of the expansion (1) should be sought experimentally. Nevertheless, it is helpful to discuss the for-

mal and physical reasons for the occurrence of excited clusters.

The appearance of excited clusters in the expansion (5) is a consequence of three factors: the presence of the average nuclear field, the effect of the Pauli principle, and the separation of the variables in the oscillator Hamiltonian of the TISM for any set of Jacobi coordinates

$$H_A(\xi_A) = H_{A-x}(\xi_B) + H_x(\xi_x) + H_{\text{rel}}(\mathbf{R}_{A-x}-\mathbf{R}_x), \quad (10)$$

where H_A, H_{A-x}, and H_x are the internal Hamiltonians of the TISM for the systems of A, $A-x$, and x nucleons; H_{rel} is the Hamiltonian that describes the relative motion of the fragments $A-x$ and x. The property (10) must be augmented by the assertion that the spectra of all three Hamiltonians H_{A-x}, H_x, and H_{rel} in the TISM are completely identical and are determined by the same parameter $\hbar\omega$. The first two factors lead to the appearance of excitation quanta in the system of A nucleons. And by virtue of the third property these quanta can be transferred without hindrance from one subsystem to the other or pass into their relative motion. It is this fact that is established in the oscillator rule (6) and in the summation over the oscillator quanta in the expansion (5). However, this last property is true only of the oscillator Hamiltonian and is not true for any other types of interaction. Does this mean that excited clusters are meaningful only in the framework of the oscillator TISM and do not appear in more realistic schemes?

To answer this question, we consider first the model of nucleon associations.[1] The wave function of a system consisting of two clusters x and B is expressed in this model in the form of an antisymmetrized product of the internal functions $\psi_x(\xi_x)$ and $\psi_B(\xi_B)$ of the clusters and the function $\psi_{\nu\Lambda}(\rho)$ of their relative motion:

$$\psi_A(\xi_x, \xi_B, \rho) = N\hat{A}_{xB}\{\psi_x(\xi_x)\psi_B(\xi_B)\psi_{\nu\Lambda}(\rho)\}. \quad (11)$$

Here, the clusters x and B are taken in the ground states, and the number of nodes of the function $\psi_{\nu\Lambda}(\rho)$ is chosen in accordance with the oscillator rule (6) for $N_x = N_x^{\min}$, $N_B = N_B^{\min}$. If all three functions in (11) are oscillator functions and are characterized by the same oscillator parameter $\hbar\omega$, then, as is well known,[32] the function (11) is identical to the TISM shell function (5). In other words, as a result of the exchange of nucleons between the unexcited clusters realized by the antisymmetrization operator $\hat{A}_{xB}$, excited clusters appear in the wave function (11) just as in (5).[2)] If all three functions in the curly brackets of the expression (11) differ somewhat in the oscillator parameters, $\hbar\omega_1 \neq \hbar\omega_2 \neq \hbar\omega_3$ [in this case, the spectra of the Hamiltonians in (10) are not identical and, strictly speaking, the oscillator rule (6) is no longer justified], the excited clusters are masked in the exchange terms. If the clusters are strongly individuated (there are large differences between the quanta $\hbar\omega_1$, $\hbar\omega_2$, $\hbar\omega_3$), the antisymmetrization becomes ineffective, and the excited clusters die out in the wave function.

It is also obvious that the construction (11) does not reflect all structural details of a cluster nucleus, namely, it does not take into account the possibility of deformation or breakup of clusters in the region of strong interaction in the system of $A = x + B$ nucleons. To take into account these effects the resonating-group method introduces into the trial function (11) additional terms with excited clusters:

$$\psi_A(\xi_x, \xi_B, \rho) = \hat{A}_{xB}\{\psi_x(\xi_x)\psi_B(\xi_B)\psi_{\nu\Lambda}(\rho)\} + \sum_i \hat{A}_{xB}\{\psi_{x^*}^{(i)}(\xi_x)\psi_B(\xi_B)\psi_{\nu_i\lambda_i}(\rho)\}. \quad (12)$$

Here, $\psi_{x^*}^{(i)}(\xi_x)$ is the wave function of the excited state of cluster x, chosen orthogonal to the ground-state function ψ_x. In general, the functions of the excited states do not then correspond to any real excitations of the system of x nucleons. They represent virtual inelastic channels in the continuum. The role of these so-called breathing excitations of clusters in the ground states of the ^{6}Li and ^{7}Li nuclei was investigated in the resonating-group method in Refs. 33–35 with allowance for the coupling of the channels α–d, α–d^* and α–t, α–t^*, respectively. Variational calculations with the trial functions (12) for a Hamiltonian with realistic two-body NN interactions show that inclusion of the channel with an excited cluster x^* changes the clustering in the surface region of the nucleus only little. At the same time, the functions of the relative motion of the clusters in the channel with x^* have appreciable amplitudes in the interior region of the nucleus and agree in the number of nodes with the oscillator rule (6) for $N_x > N_x^{\min}$. Overall, the inclusion of the excited clusters improves the behavior of the wave function of the nucleus in the internal region, both through the appearance of new components in the wave function with respect to the relative coordinate and through the enhancement of the high-momentum component of the internal wave function of the cluster. As a result, it was possible to obtain[35] an appreciable enhancement of the electromagnetic form factors of the ^{7}Li nucleus in the region of large q ($\sim$10 F^{-2}), improving the agreement between theory and experiment. Thus, it may be concluded that the results of calculations in the resonating-group method confirm the main qualitative ideas about excited clusters that follow from the shell model and are used in what follows.

2. WHEN ARE EXCITED CLUSTERS MOST IMPORTANT IN NUCLEAR REACTIONS?

A qualitative answer to the question posed in the title of this section can be found in the properties of excited clusters considered above. The principal and, indeed, only advantage of excited clusters in nuclear reactions over unexcited clusters is the presence in them of a high-momentum component, especially in the single-nucleon channel $x \to (x-1) + N$ (Fig. 3). Possible processes with transfer of a fluctuation $x \to (x-1) + N$ to the mass shell under the influence of γ rays, pions, and nucleons are shown in Figs. 3(b)–3(d). If the kinematics of the reactions on nuclei corresponding to them, (γ, Nx), (π, Nx), and (p, px), are such that at the vertex $x \to (x-1) + N$ the relative momentum Q is greater than the characteristic shell value Q_0 ($Q > Q_0$), then the con-

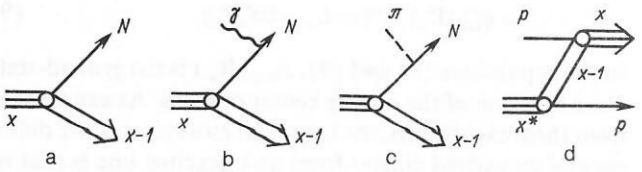

FIG. 3. Virtual decay $x \to (x-1) + N$ (a) and possible processes with its participation induced by γ rays (b), pions (c), and nucleons (d).

tribution of the excited clusters to these processes may be dominant. As estimates in the TISM without allowance for short-range correlations show, the amplitude of the process $x \to (x-1)+N$ with excited cluster $x=4$, $N_x=2$–4 for $Q=(1.5\text{–}2.0)Q_0$ exceeds by an order of magnitude the analogous amplitude for an unexcited cluster ($N_x=0$). The condition $Q>Q_0$ can be realized in (γ, Nx) and (π, Nx) reactions at large emission angles of the fragments and in quasielastic (p, px) knockout with px scattering backward. Conversely, for $Q<Q_0$ the transitions on ordinary clusters are dominant, since for them the weight of the momentum-soft components of the wave function is higher than for the excited clusters.

We consider now the possible reasons for suppression of the contribution of excited clusters. Three can be identified.

1. The first is related to the existence of the nuclear surface. Ordinary clusters are localized in the surface layer, whereas excited clusters extend into the nucleus.[3)] The continuum wave functions in the entrance and exit channels change their behavior abruptly at the boundary of the interaction potential in two respects. First, in the interaction region the oscillations of the wave function are enhanced, since for an attractive potential the wave vector k_{int} in the interaction region is greater than the asymptotic wave vector k_{out}: $K_{\text{int}} > k_{\text{out}}$. Second, the amplitude of the scattered wave is decreased in the interior region approximately in the ratio $K_{\text{int}}/k_{\text{out}} \simeq ((T+|V|)/T)^{1/2}$, where V is the depth of the potential well, and T is the kinetic energy of the particle outside the interaction region. This decrease in the wave amplitude is formally a consequence of the matching of oscillating functions with strongly differing wave vectors,[36] a mathematical operation that from the physical point of view corresponds to reflection of the wave from the surface of the attractive potential. An exception is resonance scattering, for which the wave function of the incident particles penetrates deeply into the region of the attractive potential without a decrease in amplitude. The additional damping of the wave within the nucleus is due to absorption, i.e., the imaginary part of the optical potential.

Both of these interrelated factors lead to two independent mechanisms that suppress the contribution of the excited clusters to the reaction cross section. The effect of the second factor is obvious; for the incident particles penetrate weakly within the nucleus into the localization region of the excited clusters, and the fragments $x-1$ and N formed by the interaction with the cluster undergo absorption in passing through the nucleus. The effect of the first factor can be understood, for example, in the semiclassical approximation by examining Fig. 4. In this figure, we consider two fluctuations $x \to (x-1)+N$ and $x^* \to (x-1)+N$, which occur on the surface and in the interior region of the nucleus, respectively. If the fluctuations are brought to the mass shell [for example, by any of the methods shown in Figs. 3(b)–3(d)], then for the same asymptotic relative momentum q the local relative momentum Q in the fluctuation $x^* \to (x-1)+N$ must be greater than in $x \to (x-1)+N$ by virtue of the general renormalization of the momentum in the region of attraction. In other words, under otherwise identical experimental conditions the excited clusters participate in the reaction at larger values of the momentum in the channel $x^* \to (x-1)+N$, and this lowers the amplitude of this process relative to the $x \to (x-1)+N$ amplitude. Thus, the existence of an interface between the external and internal regions of the nucleus is the main factor that suppresses the contribution of the excited clusters to the reaction cross section when allowance is made for distortions. The plane-wave calculations[37] evidently cannot pretend to even a qualitative estimate of the cross section.

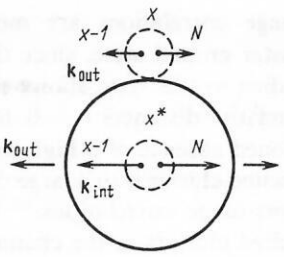

FIG. 4. Increase of the local relative momentum in the channel $x^* \to (x-1)+N$ compared with its asymptotic value in the process with participation of an excited cluster x^*.

2. Another important factor in suppressing the contribution of the excited clusters is the mechanism of the "elementary" interaction of a hadron with a cluster: $h+x \to N+(x-1)+\ldots$. The dynamics of this process may be such that even in the case of kinematic conditions favorable for manifestation of the high-momentum component of the wave function the process takes place predominantly on small relative momenta in the channel $x \to (x-1)+N$. Examples of such diagrams in the Δ-resonance region of interaction with deuterons (two-nucleon clusters) are well known[38] and are given in Fig. 5. In the first two processes, the relative momentum of the separating nucleons is fairly large. However, it does not arise because of the large relative momentum at the vertex $\langle 2N \rangle \to N+N$, whose probability is small, but because of the large probability for production of the Δ isobar and its subsequent "explosion," which is what repels the originally slow nucleons. For the same reason, soft momenta are dominant in the $p\langle np \rangle \to pd$ process in the vertices $\langle 2N \rangle \to N+N$ and $p+n \to d$.[41] The diagrams shown in Fig. 5 are dominant in the region of energies for which the Δ isobar is near the mass shell. Outside the Δ-resonance region the mechanisms shown in Fig. 3, which require high-momentum components of the wave functions, become important. Analogous conclusions hold for processes involving more complicated clusters (see Sec. 3).

3. Finally, there is one further important aspect of the competition between the excited and unexcited clusters; it is related to the short-range correlations in the channel x

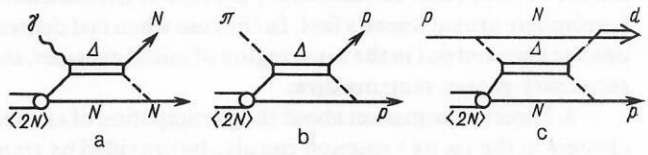

FIG. 5. Examples of processes on a $\langle 2N \rangle$ cluster that can be realized without participation of high-momentum components in the channel $2N \to N+N$: (a) photodisintegration of the "deuteron," $\gamma\langle 2N \rangle \to NN$, at γ-ray energy $E_\gamma \sim 200$–300 MeV (Ref. 39); (b) absorption of stopped pions, $\pi\langle 2N \rangle \to NN$ (Ref. 40); (c) proton backward scattering in the process $p\langle 2N \rangle \to Nd$ at initial proton energy $T \sim 500$–700 MeV.[41]

$\to (x-1)+N$. The short-range correlations are most strongly manifested in the cluster ground state, since the configuration $(0s)^x$ corresponding to this state allows the nucleons to approach to short relative distances $r_{ij} \sim 0$. Because of this, the above-mentioned absence of a high-momentum component in an unexcited cluster is to a large degree compensated by the short-range correlations.[42] In contrast, their influence in excited clusters in the channel $x^* \to (x-1)+N$ is less significant precisely on account of the admixture of the high shell configurations $s^{x-1}p^1$,..., $s^{x-1}(N_xL_x)^1$, in which the average distance between a nucleon in the N_xL_x shell and the core s^{x-1} is appreciably greater than the dimension of the core s^{x-1}. The problem of the influence of the short-range correlations in the ground state of a cluster s^x was actually considered in Ref. 43 in an analysis of p^3He and p^4He backward elastic scattering in the framework of the heavy-stripping mechanism at energies 600 MeV. It was established that allowance for the short-range correlations in the channel $x \to (x-1)+N$ reduces approximately to multiplication of the oscillator function $\psi_{000}(\rho)$ by a correlation function $u(\rho)$ having the form

$$u(\rho) = 1 - a \exp\left\{-b\left(\frac{x-1}{x}\right)^2 \rho^2\right\}, \qquad (13)$$

where ρ is the distance between the centers of mass of the core $x-1$ and the nucleon. The parameters a and b in (13) were chosen to satisfy the condition of describing the charge form factors of the ^{3}He and ^{4}He nuclei: $a_{^3\mathrm{He}} = 0.2$, $b_{^3\mathrm{He}} = 4.65\ \mathrm{F}^{-2}$, $a_{^4\mathrm{He}} = 0.43$, $b_{^4\mathrm{He}} = 0.708\ \mathrm{F}^{-2}$. The same correlation function (13) is used to estimate the short-range correlations in excited clusters.[42] From the given treatment, the following conclusions can be drawn about the conditions favorable for the manifestation of excited clusters in quasielastic knockout reactions.

1. A necessary condition for a large contribution of excited clusters to the reaction cross section is a large relative momentum at the vertex $x^* \to N + (x-1)$. In a QKNC reaction of the (p, px) type, this condition can be realized if protons are emitted backward, since in this case a large contribution of the pole diagram in the $px^* \to px$ process is possible [see Fig. 3(c)].

2. It is important for the energies of the particles in the entrance and exit channels to be sufficiently high. This reduces the wave-vector ratio $K_{\mathrm{int}}/k_{\mathrm{out}}$ (for $T = 600$ MeV, $V = 100$ MeV, we have $K_{\mathrm{int}}/k_{\mathrm{out}} \simeq 1.1$), and this also reduces the effect of the nuclear surface as a factor that suppresses the contribution of the excited clusters. This condition is satisfied by the $(p, p^3\mathrm{H})$, $(p, p^3\mathrm{He})$, and $(p, p^4\mathrm{He})$ reactions at large momentum transfer in the region of energies around 1 GeV, at which not only the clusters knocked out forward but also the secondary protons in the backward hemisphere are sufficiently fast. In the case when fast deuterons are knocked out in the same region of initial energies, the secondary proton remains slow.

3. Direct information about the participation of excited clusters in the (p, px) reaction can also be provided by transitions to states of the residual nucleus that are forbidden (in the impulse approximation) in the case of knockout of unexcited clusters. Such are, for example, transitions to levels of the residual nucleus with isospin $T_B = 1$ in the case of α-particle knockout from a target nucleus with isospin $T_A = 0$.

It is also obvious that QKNC reactions at high initial energies but small momentum transfers do not completely satisfy these conditions. First, the knocked-out cluster remains slow and is strongly absorbed in the nucleus. Second, in the limit of zero momentum transfer, $\Delta \to 0$, the Glauber multiple-scattering diagram for the $px^* \to px$ process vanishes because the states of the excited and unexcited clusters are orthogonal. (Actually, the amplitude is not zero only because of the differences between the oscillator parameters of the free cluster and the cluster bound in the nucleus.) Third, the Glauber scattering operator is diagonal with respect to the cluster Young diagram $[f_x]$. Therefore, when three- and four-nucleon clusters are knocked out at $\Delta \sim 0$ the permutational symmetry of the cluster, $[f_x] = [3]$ or $[4]$, cannot change, and, as a consequence of this, the value of the isospin T_x cannot change (see the final paragraph of the subsection "Properties of excited clusters").

3. BACKWARD ELASTIC SCATTERING OF PROTONS BY THE LIGHTEST NUCLEI AT INTERMEDIATE ENERGIES

We consider briefly pd, p^3He, and $p\alpha$ backward elastic scattering at energies of several hundred mega-electronvolts. A general theory of backward elastic scattering of fast protons by nuclei has not yet been created, and it is clear that it cannot be as comparatively simple and universal as, for example, the Glauber–Sitenko theory of multiple scattering, which is valid at small momentum transfers Δ. The construction of a corresponding theory at large Δ encounters the problems of the high-momentum components of the nuclear wave functions, the non-nucleon degrees of freedom in nuclei, and the relativistic description of bound states of hadronic systems, i.e., the most topical problems in the theory of strong interactions quite generally. Mechanisms of proton backward scattering by light nuclei are considered here not so much to demonstrate the full complexity of this problem but mainly with a view to answering schematically the question of the contribution of excited $\langle 2N\rangle$, $\langle 3N\rangle$, and $\langle 4N\rangle$ clusters to the kinematically corresponding "elementary" processes in QKNC reactions.

Backward elastic *pd* scattering

Of the processes listed above, the best studied is pd backward scattering in the region of initial energies $T_p = 0.2$–2.5 GeV. However, even in this simplest case the interaction mechanism cannot be regarded as definitively clarified. It has been shown that in the region of energies 500–700 MeV the triangle diagram of one-pion exchange (OPE) with virtual subprocess $pp \to d\pi^+$ can be expected to make a large contribution to the pd scattering cross section due to the Δ-resonance maximum of the $pp \to d\pi^+$ process at energy $T_p = 600$ MeV (Fig. 6a).[44,45] This mechanism reproduces the energy and angular dependences of the cross sec-

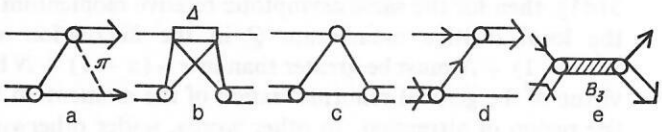

FIG. 6. Mechanisms of elastic pd backward scattering: (a) one-pion exchange; (b) the Δ-resonance mechanism; (c) single scattering; (d) single-nucleon exchange; (e) mechanism with formation of a B_3 resonance.

tion in the considered interval of energies. However, for a clearer understanding of the Δ-resonance behavior of the $pd \to dp$ cross section, it is necessary to consider diagrams that explicitly include the Δ isobar in the intermediate state. One of these diagrams, shown in Fig. 6(b), was considered in Refs. 41 and 46. The results of calculation with the Δ isobar are not sensitive in this region to the high-momentum component of the deuteron (see Sec. 2) but depend strongly on the parameters of the $NN \leftrightarrows N\Delta$ transition amplitudes, which are calculated in the approximation of $\pi + \rho$ meson exchange and are known, unfortunately, with low accuracy. The inclusion in the Δ-resonance mechanism of the diagrams of single scattering [Fig. 6(c)] and neutron exchange [Fig. 6(d)], which are very sensitive to the high-momentum component of the deuteron, hardly changes the absolute value of the cross section in this region of energies, although it does affect the polarization characteristics. According to Ref. 46, the sum of the three diagrams of Figs. 6(b), 6(c), and 6(d), calculated with a realistic deuteron function in the Reid potential with a soft core with allowance for the relativistic effects in the dynamics on the light cone,[48] cannot reproduce all the existing experimental data even when the $\pi N\Delta$ and $\rho N\Delta$ vertex constants are varied arbitrarily. For example, the characteristic "shoulder" at energy 500–600 MeV in the cross section of scattering through angle $\theta_{\text{cms}} = 180°$, which is traditionally regarded as a manifestation of the Δ-resonance feature, is only partly reproduced. In this connection, it was suggested in Ref. 47 that in this region of energies there is a large admixture of a mechanism with intermediate production of three-baryon resonances B_3 [Fig. 6(e)], whose existence in this region of energies can in fact be justified in the bag model.[49] The parameters of the B_3 resonances in the Breit–Wigner form can be chosen in such a way that the sum of the four diagrams of Figs. 6(b), 6(c), 6(d), and 6(e) describes the experimental data, including the deuteron tensor polarization.[50] It should be noted that the predictions of the OPE mechanism[46] contradict the new data on the tensor polarization.[51]

At energies of the incident protons above 1 GeV, the contribution of the Δ and B_3 resonance mechanisms decreases rapidly, while the contribution of the mechanism of neutron exchange and single scattering increases. On the basis of the so-called optimal approximation developed in Refs. 52 and 53—it is a generalization of the impulse approximation to the case of large momentum transfers—it was shown that in the region of energies 1–2 GeV the sum of the mechanisms of neutron exchange and single scattering with allowance for rescattering in the entrance and exit channels explains the energy and angular dependences of the backward scattering cross section.[54] It should, however, be noted that the approach of Refs. 52–54 is dynamically nonrelativistic. At energy $T_0 = 2.5$ GeV a resonance feature is again observed; it is apparently associated with double excitation of the Δ isobar.[55]

Leaving on one side the question of the exact contribution of each of the considered mechanisms, we can conclude that in the quasifree process $p\langle 2N\rangle \to Nd$ transitions with excited $\langle 2N\rangle$ clusters will be most important in the region of energies 1–2 GeV. In contrast, at energies 500–800 MeV the contribution of such transitions is strongly suppressed. For this assertion, we have the following arguments, which have already been established in the OPE approximation.[45] First, the Δ and, evidently, B_3 resonance mechanisms are not sensitive to the high-momentum component of the wave function of an NN pair, and therefore the dominant contribution to the cross section of the (p, pd) reaction will be made by states with internal orbital angular momentum $l = 0$ of the pair. Second, for the Δ resonance and OPE mechanism the probability of a transition with a change of the pair isospin, $pd^*_{T=1} \to pd_{T=0}$, is suppressed by nine times compared with the transition $pd_{T=0} \to pd_{T=0}$ without change in the isospin if, in accordance with the TISM, it is assumed that the spatial functions of the singlet, $d^*_{T=1}$, and triplet, $d_{T=0}$, deuterons are the same.

Elastic $p\alpha$ and p^3He backward scattering

In the literature there are some examples of good fitting to the data on elastic $p\alpha$ backward scattering in the framework of the DWBA at initial energies 100–150 MeV (Ref. 56) and in the region 400–800 MeV.[57,58] The main feature of the scattering process in these energy intervals—the growth of the c.m.s. cross section as the scattering angle approaches 180°—is well reproduced by the Majorana (space-exchange) part of the optical potential, this corresponding in the language of Feynman diagrams to the triton exchange mechanism [Fig. 7(b)]. Relativization of the exchange term[58] does not change these results qualitatively. To describe the α particle in the virtual-decay channel $\alpha \to t + p$ in such calculations one uses a simple functional form of the type of Eckart parametrization.[57] The unknown parameters of this wave function are chosen by fitting to the binding energy in the $\alpha \to t + p$ channel and the charge form factor $F_\alpha(q)$ in a wide range of momentum transfers. Elastic $p\alpha$ backward scattering with an s-wave function $\psi(\mathbf{q})$ corrected to take into account the contribution of the meson exchange currents to $F_\alpha(q)$ was analyzed in Ref. 59. In this work, two mechanisms were summed in the optical model—single scattering [Fig. 7(a)] and heavy stripping [Fig. 7(b)] with allowance for rescatterings. The calculated curves obtained in Ref. 59 agree well with the data on the angular and energy dependences of the backward scattering cross section in the interval 100–800 MeV except for the region 200–400 MeV.

In the region of energies 200–400 MeV there is an appreciable discrepancy between the model of Refs. 57 and 59 and experiment,[60] namely, the observed differential cross section of backward scattering ($\theta_{\text{cms}} = 160$–$180°$) is practically isotropic, and the deep dip in the energy dependence of the scattering cross section at angle $\theta_{\text{cms}} = 180°$ which is predicted by the triton exchange mechanism[57] and is partly filled by the summation of the diagrams of Figs. 7(a) and 7(b)[59] is absent experimentally.[16] The data on the polarization of the protons in this region of energies also contradict the model of Ref. 59. In the opinion of the present authors,

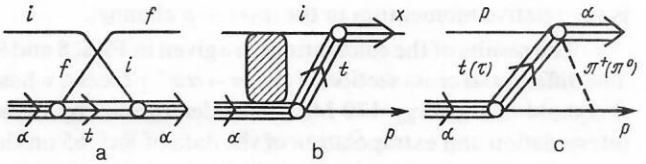

FIG. 7. Mechanisms of elastic $p\alpha$ backward scattering: (a) single scattering; (b) heavy stripping with allowance for distortions (exchange of a tritium nucleus); (c) triangle diagram of one-pion exchange.

all this indicates that the other possible scattering mechanisms make an important contribution in this region of energies. To this end, we considered in Refs. 60 and 61 the triangle diagram with the virtual subprocess $p + t(\tau) \to \alpha + \pi$ [Fig. 7(c)]. The contribution of this diagram can be appreciable precisely in the interval 200–400 MeV, since according to the estimates of Ref. 62 the Δ-resonance maximum of the $p + t \to \alpha + \pi$ process is expected at energies 300–350 MeV.

By analogy with Refs. 44 and 45, the $p\alpha$ scattering cross section can be expressed in the framework of the OPE mechanism in terms of the differential cross section of the $p + \tau \to \alpha + \pi$ process[61]:

$$\frac{d\sigma^{p\alpha\to\alpha p}}{d\Omega_\theta} = 3\,\frac{G^2}{4\pi}\,F^2(k^2)\,\frac{T_p + 2m_p}{(T_p + m_p)^2} \times \frac{m_\alpha}{m_\tau}\,\frac{s_{p\tau}}{s_{p\alpha}}\,J(Q,\varkappa)\,\frac{d\sigma^{p\tau\to\alpha\pi^+}}{d\Omega_\varphi}, \qquad (14)$$

where

$$J(Q,\varkappa) = \int_0^\infty j_1(Q\rho)\,(\varkappa\rho + 1)\exp(-\varkappa\rho)\,\psi(\rho)\,d\rho. \qquad (15)$$

Here and in what follows, m_i is the mass of particle i; s_{ij} and q_{ij} are the square of the total energy of particles i and j in the system of their common center of mass and the relativistic momentum of the relative motion, respectively; $G^2/4\pi = 14.7$; $F(k^2)$ is the Ferrari–Selleri form factor[63]; k^2 is the square of the 4-momentum of the virtual pion; and T_p is the kinetic energy of the secondary proton. The connection between $\cos\varphi$ and $\cos\theta$ is determined by analogy with Ref. 64. The relativistic expressions for T_p, Q, and $\varkappa$ are determined as in the case of pd scattering.[45] The wave function $\psi(\rho)$ describes the s state of relative motion at the virtual decay vertex $\alpha \to p + t$ (or $\alpha \to n + \tau$); $j_l(x)$ is the spherical Bessel function of order l. For comparison, we note that in the framework of the single-scattering mechanism the cross section is proportional to the square of the α-particle elastic form factor $S(\Delta)$:

$$S(\Delta) = \int_0^\infty j_0\left(\frac{3}{4}\,\Delta\rho\right)\psi^2(\rho)\,\rho^2\,d\rho, \qquad (16)$$

where Δ is the momentum transfer in the $p\alpha \to \alpha p$ process. For the triton-exchange pole mechanism the $p\alpha$ scattering cross section is proportional to the fourth power of the wave function in the $\alpha \to t + p$ channel in the momentum representation,

$$\psi(q) = \int_0^\infty j_0(q_{pt}\rho)\,\psi(\rho)\,\rho^2\,d\rho, \qquad (17)$$

where

$$q_{pt} = \left\{\frac{(p_t p_p)^2 - m_t^2 m_p^2}{(p_t + p_p)^2}\right\}^{1/2} \qquad (18)$$

is the relative momentum in the $\alpha \to t + p$ channel.

The results of the calculations are given in Figs. 8 and 9. The differential cross section of the $p\tau \to \alpha\pi^+$ process, whose threshold is at energy 170 MeV, was determined by linear interpolation and extrapolation of the data of Ref. 65 on the inverse reaction $\pi^-\alpha \to nt$. For all mechanisms, the wave function $\psi(\rho)$ in the Eckart parametrization[57] was used. The presence of the deep minimum in the charge form factor

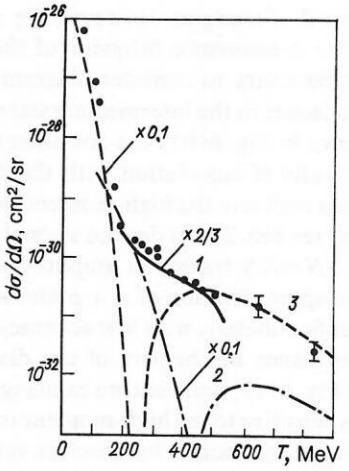

FIG. 8. Differential cross section of elastic $p\alpha$ scattering in the center-of-mass system through angle $\theta_{cms} = 180°$ as a function of the initial kinetic energy: (1) OPE; (2) single scattering; (3) heavy stripping. The experimental points are taken from Ref. 60. Curves 2 and 3 are multiplied by the factor 0.1.

$F_\alpha(q)$ at $q = 3.2$ F^{-1} leads to vanishing of $\psi^2(q_{pt})$ and $S^2(\Delta)$ at initial energies 240 and 440 MeV ($\varphi_{cms} = 180°$), respectively. Because of this, the contribution of the pole mechanism is suppressed in the region of energies 200–400 MeV (curve 3), and the single-scattering diagram predicts an excessively rapid decrease of the cross section compared with the experiment (curve 2). (In Fig. 8, curves 3 and 2 are normalized to the experiment at energies T_p equal to 100 and 200 MeV, respectively; the normalization factor is 10^{-1}, corresponding to the contribution of the absorptive distortions in this region.[57]) In contrast, the integral $J(Q,\varkappa)$ in (15) is a smooth function of the kinematic variables, and, as can be seen from Figs. 8 and 9, the OPE mechanism leads to a correct qualitative and quantitative description of the energy and angular dependences of the $p\alpha$ backward scattering cross section in the region of energies 200–450 MeV. To describe the analyzing power of the $p\alpha \to \alpha p$ process, it is necessary to investigate the interference between the mechanisms shown in Fig. 7, and for this it is necessary to know the

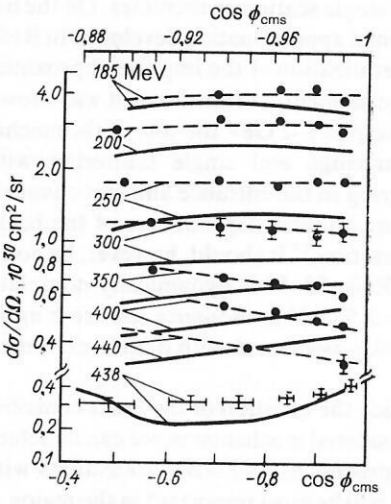

FIG. 9. Differential cross section of elastic $p\alpha$ scattering in the center-of-mass system at different energies of the initial particle. The calculation (continuous curves) in accordance with Eq. (14) is compared with experiment[60] (points and broken lines) according to the upper scale and at $T = 438$ MeV according to the lower scale.

amplitude of the $p\tau \to \alpha\pi^+$ process. The summation of the diagrams of Figs. 7(b) and 7(c) requires care, since one of them already includes the other (at least partly) by virtue of the triton pole in the amplitude of the $p\tau \to \alpha\pi^+$ process. At energies above 500 MeV, this mechanism becomes unimportant because of the rapid decrease of the cross section of the $p\tau \to \alpha\pi^+$ process.

The characteristic feature of these models is the use of a phenomenological function in the $\alpha \to t + p$ channel fitted to the α-particle charge form factor. Despite the serious shortcomings of such fitting (in particular, the neglect of the $\alpha \to p + \langle 3N \rangle$ channel, where the state $\langle 3N \rangle$ is not the tritium nucleus), it is important that through the introduction of the phenomenological s-wave function in the $\alpha \to t + p$ channel it is possible to describe the charge form factor $F_\alpha(q)$ in the interval $q = 0$–$7\ \mathrm{F}^{-1}$ and, at the same time, to understand the basic features of $p\alpha$ backward scattering at large momentum transfers. It has been recently established[59,66] that fitting directly to the experimental charge form factor $F_\alpha^{\exp}(q)$ raises the values of the function $\psi_{\alpha \to t+p}(q)$ by 1.5–2 times in the interval of momenta $q = 2$–$4\ \mathrm{F}^{-1}$, since this procedure does not take into account the contribution of the meson exchange currents to $F_\alpha^{\exp}$. It is important that the appropriate correction of the function $\psi_{\alpha \to t+p}$, to take into account the contribution of the meson exchange currents to $F_\alpha^{\exp}$, improves, for example, the description of the $^4\mathrm{He}(p, d)^3\mathrm{He}$ reaction in the single-nucleon exchange model with distortions at energies 400–700 MeV (Ref. 67) and, as follows from Ref. 59, does not change the qualitative conclusion[57] about the part played by the single-scattering and heavy-stripping mechanisms in $p\alpha$ backward scattering. The OPE diagram is practically insensitive to such a correction of the function. It is known[68] that calculations with realistic three- and four-nucleon wave functions do not reproduce the charge form factors of the ^{3}He and ^{4}He nuclei in the region of the second maximum even when allowance is made for the meson exchange currents and three-particle forces. This result is attributed to the contribution of the non-nucleon components of the nuclear wave functions. A positive aspect of the phenomenological fitting to the charge form factor is the possibility of taking this contribution into account. At the same time, it should be noted that the available data on $p\alpha$ backward scattering up to the energy $T_p = 1000$ MeV correspond to values of the square of the momentum transfer $q^2 \leqslant 5.3\ \mathrm{GeV}^2/c^2$. This value significantly exceeds the maximal momentum transfer $q^2 = 2.4\ \mathrm{GeV}^2/c^2$ achieved in the data on electron scattering by α particles.[69] In proton scattering through angle $\theta_{\mathrm{cms}} = 180°$, a momentum transfer $q^2 = 2.4\ \mathrm{GeV}^2/c^2$ is attained already at energy $T_p = 500$ MeV. Therefore, elastic $p\alpha$ backward scattering at $T_p > 500$ MeV may contain new information about the high-momentum components of the α-particle wave function compared with the data on the charge form factor. Calculations of the characteristics of this process with realistic four-nucleon wave functions of the α particle are at present unavailable.

Information about the mechanisms of p^3He scattering into the backward hemisphere is more sparse than in the case of pd or $p\alpha$ scattering. The calculations of Ref. 70, made in the framework of the deuteron exchange mechanism with a phenomenological s-wave function in the $^3\mathrm{He} \to d + p$ channel in the Eckart parametrization, do not explain the data in the interval 400–600 MeV, in contrast to the analogous model of $p\alpha$ scattering. One of the reasons for this is the neglect of the D-wave contribution in the $^3\mathrm{He} \to d + p$ channel, which, in contrast to the $\alpha \to t + p$ channel, is not forbidden by the angular-momentum conservation law. The part played by the $d + p$ configuration of the ^{3}He nucleus was investigated in Ref. 71 on the basis of the overlapping of the realistic three-body function of the ^{3}He nucleus from the Faddeev equations and the deuteron function, these functions being obtained for the potential of the NN interaction in Reid's form with a soft core with allowance for the S and D waves in both nuclei.[72] If the weight of the $d + p$ configuration in the ^{3}He nucleus is normalized to unity, then in such calculations it is possible to describe the charge form factor of the ^{3}He nucleus up to values of the momentum transfer $q = 7\ \mathrm{F}^{-1}$ to the accuracy inherent in the impulse approximation (without allowance for the meson exchange currents) and, at the same time, to explain on the basis of the deuteron exchange mechanism the break in the energy dependence of the p^3He scattering cross section at angle $\theta_{\mathrm{cms}} = 180°$ in the region of energies $T_p = 400$–600 MeV. The contribution of the single-scattering mechanism in the region of energies $T_p = 400$–700 MeV is negligibly small, owing to the second (theoretical) minimum in the charge form factor of the ^{3}He nucleus. In the region of energies 700–1700 MeV, where the momentum transfer reaches values $q = 7$–$15\ \mathrm{F}^{-1}$, the restriction to the $d + p$ configuration of the ^{3}He nucleus in treating the heavy-stripping and single-scattering mechanisms, which require high-momentum components of the wave function, becomes unjustified in accordance with the results of the description of the charge form factor. Corresponding calculations outside the framework of the $d + p$ approximation have not yet been made in this kinematic region. Calculations on the basis of the OPE mechanism with the virtual subprocess $pd \to t\pi$ (Ref. 71) predict in the energy interval 400–1700 MeV a cross section that is approximately an order of magnitude lower than the experimental cross section.

It follows from the treatment given that in the backward elastic scattering of fast protons by the lightest nuclei the exchange interaction mechanisms play the principal role; as a result of these, there appears in the final state a proton that originally belonged to the target nucleus, in which its place is taken by the incident proton. In classical language, this means that in backward elastic scattering the target nucleus is broken up but a new nucleus of the same kind is formed by capture of a group of nucleons by the fast incident proton, which preserves its direction of motion. From the point of view of these mechanisms, the process of rearrangement of the internal structure of the cluster, $px^* \to px$, appears most natural.

4. CALCULATIONS OF THE CHARACTERISTICS OF QKNC REACTIONS WITH ALLOWANCE FOR EXCITED CLUSTERS

Elements of the formalism

The calculations given below of the basic characteristics of QKNC reactions $A(p, Nx)B$ are based on the impulse approximation, the validity of which at high energies is not in doubt.

It is well known that in the ordinary approaches without allowance for excited clusters the QKNC cross section in

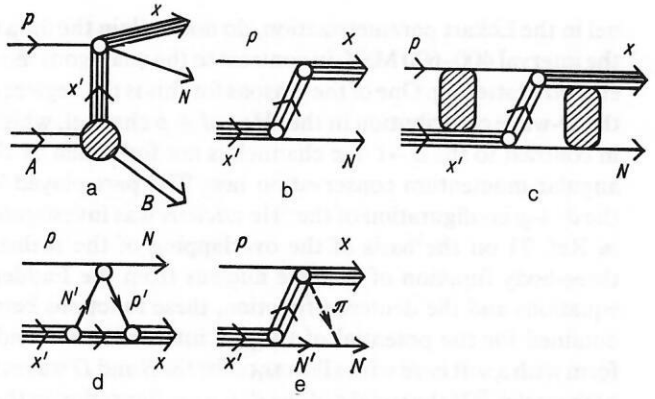

FIG. 10. Amplitude of the quasielastic knockout reaction $A(p, Nx)B$ with the participation of excited clusters x' (a) and mechanisms of the quasifree process $px' \to Nx$: (b) heavy stripping; (c) heavy stripping with allowance for distortions; (d) single pN scattering; (e) one-pion exchange.

the impulse approximation with either plane[1] or distorted waves can be factorized into the following factors: a structure factor, which depends on the wave functions of the initial and final nuclei, the momentum distribution of the knocked-out cluster in the target nucleus, and the cross section of inelastic scattering of the incident protons by the free cluster. When the excited clusters are taken into account, such a factorization does not hold. In this case, the amplitude T_{fi} of the quasielastic knockout reaction is actually the interfering sum of pole diagrams (Fig. 10) for different internal states of the knocked-out clusters and different states of the relative motion of the fragments x and B in the initial nucleus. In considering the amplitudes of the elementary processes, we assume, for example, that the quasifree interaction $px' \to px$ can, irrespective of the internal state of the knocked-out particles, be described by the same mechanism as free $px \to px$ scattering in the corresponding kinematic region and that the spin–isospin factors that appear in these cases can be taken into account exactly.

Following Refs. 73 and 74, we represent the matrix element of the reaction $A(p, px)B$ in the form

$$T_{fi} = \binom{A}{x}^{1/2} \sum_{x,'\,\nu\Lambda} \langle \psi_A | \psi_B \psi_{x'},\ \psi_{\nu\Lambda} \rangle \Phi_{\nu\Lambda}(\mathbf{k}_B)\, T^{px' \to Nx}. \quad (19)$$

Here,

$$T^{px' \to Nx} = \langle \mathbf{k}_N \mathbf{k}_x \chi_N \psi_x | \tau(px' \to Nx) | \mathbf{k}_p,\ -\mathbf{k}_B \chi_p \psi_{x'} \rangle \quad (20)$$

is the matrix element of the $px' \to Nx$ process. In treating it, we ignore the off-shell behavior of the cluster x in the nucleus; this is the usual approximation in the theory of QKNC reactions if the energy of the incident proton significantly exceeds the binding energy of the cluster in the nucleus.[9,75] The overlap integral $\langle \psi_A | \psi_B \psi_{x'}, \psi_{\nu\Lambda} \rangle$ is the structure factor determined by Eqs. (2) and (7). The index x' labels the states of the virtual cluster x in the nucleus, and $\Phi_{\nu\Lambda}(k)$ is the momentum distribution of the cluster (or residual nucleus B) in the target nucleus A modified by the interaction in the entrance and exit reaction channels,

$$\Phi_{\nu\Lambda}(\mathbf{k}_B) = (2\pi)^{-3/2} \int \chi^{(-)*}_{xB}(\mathbf{r},\ \mathbf{k}_{xB}) \times \chi^{(-)*}_{NB}(\mathbf{r},\ \mathbf{k}_{pB})\, \psi_{\nu\Lambda}(\mathbf{r})\, \chi^{(+)}_{pA}\left(\frac{B}{A}\mathbf{r},\ \mathbf{k}_{pA}\right) d^3\mathbf{r}, \quad (21)$$

where $\chi^{(\pm)}$ are distorted waves in the two-particle channel. The optical model is usually employed to find the distorted waves. However, at high energies of the incident protons and the knocked-out clusters use of the optical model entails appreciable difficulties. The numerical solution of the Schrödinger equation with an optical potential requires much computing time, since with increasing energy the convergence of the expansion with respect to the partial waves deteriorates, and it is necessary to retain terms with orbital angular momenta up to $l \sim 100$.

We calculated the function $\Phi_{\nu\Lambda}(\mathbf{k})$ in the case of knockout of the ^{3,4}He and ^{3}H nuclei by analogy with Ref. 76 with allowance for the distortions in the entrance and exit reaction channels in the impulse representation in the language of the amplitudes of pA, pB, and xB scattering treated in the Glauber–Sitenko multiple-scattering approximation.[77] In this case, assuming that the nucleon density of the nuclei has a Gaussian shape, and ignoring the excitation of the colliding fragments in the intermediate states, we can express the function $\Phi_{\nu\Lambda}(\mathbf{k})$ in the following manner in terms of the known parameters of the amplitude of NN elastic scattering and the dimensions of the nuclei[73]:

$$\begin{aligned}
\Phi_{\nu\Lambda}(\mathbf{k}_B) = \psi_{\nu\Lambda}(\mathbf{k}_B) &+ \frac{i}{4\pi k_{pA}} \int d^2\mathbf{q}_p F_{pB}(\mathbf{q}_p)\, \psi_{\nu\Lambda}(\mathbf{k}_B - \mathbf{q}_p) \\
&+ \frac{i}{4\pi k_{NB}} \int d^2\mathbf{q}_N F_{NB}(\mathbf{q}_N)\, \psi_{\nu\Lambda}(\mathbf{k}_B - \mathbf{q}_N) \\
&+ \frac{i}{4\pi k_{xB}} \int d^2\mathbf{q}_x F_{xB}(\mathbf{q}_x)\, \psi_{\nu\Lambda}(\mathbf{k}_B - \mathbf{q}_x) \\
&- \frac{1}{(4\pi)^2 k_{pA} k_{NB}} \int d^2\mathbf{q}_p\, d^2\mathbf{q}_N F_{pB}(\mathbf{q}_p) \\
&\quad F_{NB}(\mathbf{q}_N)\, \psi_{\nu\Lambda}(\mathbf{k}_B - \mathbf{q}_N - \mathbf{q}_p) \\
&- \frac{1}{(4\pi)^2 k_{pA} k_{xB}} \int d^2\mathbf{q}_p\, d^2\mathbf{q}_x F_{pB}(\mathbf{q}_p) \\
&\quad F_{xB}(\mathbf{q}_x)\, \psi_{\nu\Lambda}(\mathbf{k}_B - \mathbf{q}_p - \mathbf{q}_x) \\
&- \frac{1}{(4\pi)^2 k_{xB} k_{NB}} \int d^2\mathbf{q}_x\, d^2\mathbf{q}_N F_{xB}(\mathbf{q}_x) \\
&\quad F_{NB}(\mathbf{q}_N)\, \psi_{\nu\Lambda}(\mathbf{k}_B - \mathbf{q}_p - \mathbf{q}_N) \\
&- \frac{i}{(4\pi)^3 k_{pA} k_{xB} k_{NB}} \int d^2\mathbf{q}_p\, d^2\mathbf{q}_N\, d^2\mathbf{q}_x \\
&\times F_{pB}(\mathbf{q}_p) F_{NB}(\mathbf{q}_N) F_{xN}(\mathbf{q}_x)\, \psi_{\nu\Lambda}(\mathbf{k}_B - \mathbf{q}_p - \mathbf{q}_N - \mathbf{q}_x).
\end{aligned} \quad (22)$$

The first term in this expression is the momentum distribution in the plane-wave approximation, and the remaining terms take into account single, twofold, and threefold rescattering in the entrance and exit channels; $F_{ij}(\mathbf{q})$ is the Glauber amplitude for scattering of particle i by the particle (nucleus) j. This method can also be used to take into account the distortions in the elementary $px' \to px$ process [Fig. 10(c)].

A different situation with regard to the allowance for distortions arises in reactions involving the quasielastic knockout of fast deuterons, for example, in the case considered below of the target nucleus ^{12}C. Here, the energy of the secondary proton, $T_p \sim 60$ MeV, is too low to permit use of multiple-scattering theory. At the same time, the high energies of the incident proton and the knocked-out deuteron, $T \sim 600$–700 MeV, make the use of the optical model diffi-

cult too. Therefore, for deuteron knockout reactions we took into account the interaction in the initial and final states in two different ways. First, following Refs. 78–80, we used the strong-absorption model, the essence of which consists of introducing cutoff radii R_0 for all integrals containing initial and final plane waves. By doing this, we get hold of the main feature in the change in the behavior of the continuum wave function at the limit of the range of the attractive potential, namely, the abrupt enhancement of the oscillations and the simultaneous decrease in the amplitude of the wave function in the internal region[81]; both these factors significantly reduce the contribution from the internal region of the nucleus.

In a different way of taking into account the distortions one uses the eikonal approximation in the simplified form of McCarthy[82] in which the distorted wave is written in the form

$$\chi^{(\pm)}(\mathbf{r},\ \mathbf{k}) = \exp\ (-\varkappa Rk)\ \exp\ [\mathrm{i}\ (1+\delta \pm \mathrm{i}\varkappa)\ \mathbf{kr}]. \quad (23)$$

Here, δ and $\varkappa$ are assumed to be independent of r and are calculated, respectively, from the real and imaginary parts of the optical potential, while R is determined by the radius of the nucleus. The function (23) is essentially a plane wave with renormalized momentum $\mathbf{k}(1+\delta)$ weakly modulated by the factor $\exp(\pm\varkappa\mathbf{k}\cdot\mathbf{r})$. It describes comparatively well the scattering of clusters by nuclei at low energies,[83] when the surface processes are dominant.

For comparison, we also give some of the calculations in the plane-wave approximation; this makes it possible to follow a feature noted in Sec. 3, namely, the different degree of influence of the distortions on the contributions of the excited and unexcited clusters.

Characteristics of *A(p, Nx)B* reactions

In the analysis of QKNC reactions, one usually considers the angular correlation function and the energy distribution of the emitted particles for transitions to a fixed state (or interval of states) of the residual nucleus, and also the excitation spectrum of the residual nucleus.[1] When the incident beam and the target nucleus are not polarized and the polarization of the final products is not detected, the invariant cross section of the $A(p, Nx)B$ reaction is given by[84]

$$d\sigma = (2\pi)^4\,\delta^{(4)}(\mathscr{P}_i - \mathscr{P}_f)\,\frac{E_pE_A\,\overline{|T_{fi}|^2}\,d^3\mathbf{k}_N\,d^3\mathbf{k}_x\,d^3\mathbf{k}_B}{[(E_pE_A - \mathbf{k}_p\mathbf{k}_A)^2 - m_p^2m_A^2]^{1/2}}, \quad (24)$$

where $E_i = T_i + m_i$ is the total energy of particle i with mass m_i, T_i is its kinetic energy, $\mathscr{P}_i$ and $\mathscr{P}_f$ are the total 4-momenta in the entrance and exit channels, respectively, and $\overline{|T_{fi}|^2}$ is the square of the reaction matrix element averaged over the initial and summed over the final spin states.

Integrating in (24) over the momentum of the residual nucleus and the kinetic energy of the knocked-out cluster x for fixed angles of the emitted particles and a definite value of the lost energy E^*, where

$$E^* = T_p - T_N - T_x - T_B - (m_x + m_B - m_A), \quad (25)$$

we obtain the energy distribution function of the secondary protons in the laboratory system ($k_A = 0$):

$$\frac{d^3\sigma}{d\Omega_N\,d\Omega_x\,dT_N} = (2\pi)^4\frac{E_pE_NE_BE_xk_N\,|\mathbf{k}_x|^2}{|R_0^N|\,|\mathbf{k}_x| - |\mathbf{R}^N|\,E_x\cos\theta\,|k_p|}\,\overline{|T_{fi}|^2}. \quad (26)$$

We have here introduced the 4-vector $R^N = \{R_0^N, \mathbf{R}^N\}$:

$$R_0^N = E_x + E_B = E_p + E_A - E_N, \quad (27)$$

$$\mathbf{R}^N = \mathbf{k}_x + \mathbf{k}_B = \mathbf{k}_p - \mathbf{k}_N, \quad (28)$$

where θ is the angle between the vectors $\mathbf{R}^N$ and $\mathbf{k}_x$. Making the change of indices $N \rightleftarrows x$ in Eqs. (26)–(28) for fixed values of the momentum $\mathbf{k}_x$ of the knocked-out fragment and lost energy E^*, we obtain the angular correlation function $d^3\sigma/d\Omega_N d\Omega_x dT_x$.

The main information about the volume distribution of the clusters in the nuclei is provided by the excitation spectra of the residual nuclei. To obtain them, it must be borne in mind that any excited state of a nucleus has a definite natural width γ_f, and the experimental energy resolution ΔE can be thought of as increasing the spreading of the levels. Therefore, the δ function in (24) that expresses the energy conservation law must be replaced by a function $\rho(E^* - E_f;\ \Delta E, \gamma_f)$, which takes into account the finite width of each level. This procedure is actually equivalent to introducing an additional integration in (19) over the energy E^* with weight function $\rho(E^* - E_f;\ \Delta E, \gamma_f)$ (where E_f is the excitation energy of the considered state of the residual nucleus) with subsequent summation over all the discrete levels E_f for the given value of the lost energy E^*. Under the condition $\Delta E \to 0$, $\gamma_f \to 0$ the density ρ takes the form $\delta(E^* - E_f)$, so that a contribution to the cross section is made by only one level, whose energy E_f is exactly equal to the value of the variable E^*; under real conditions $\Delta E \neq 0$, $\gamma_f \neq 0$ we use for $\rho(E^* - E_f;\ \Delta E, \gamma_f)$ a Gaussian form.[85]

As a result, for the excitation spectrum of the residual nucleus we obtain the expression

$$\frac{d^3\sigma}{d\Omega_x\,d\Omega_N\,dE^*} = \sum_{E_f}\int_0^{T_N^{\max}} dT_N\rho\,(E^* - E_f;\ \Delta E,\ \gamma_f)\,\frac{d^3\sigma}{d\Omega_N\,d\Omega_x\,dT_N}. \quad (29)$$

The integration in this expression is over the complete kinematically allowed interval of kinetic energies of the secondary nucleon, and the summation is over the energy levels E_f sufficiently close to E^* in an interval $|E_f - E^*| \sim \Delta E + \gamma_f$.

The $(p, p\alpha)$ reaction

The application to QKNC reactions of the formalism presented in the previous sections is considered below for the $(p, p\alpha)$ reaction at a proton energy around 700 MeV and for scattering angles near 180° in the center-of-mass system. Allowance is made for the de-excitation of the $\langle 4N\rangle$ clusters in the quasifree process

$$p + \langle 4N\rangle \to \alpha + p. \quad (30)$$

The large momentum transfer, accompanied in the general case by a change of both the spatial and the spin–isospin parts of the cluster wave function, is treated here in the framework of three Feynman diagrams: the pole diagram of heavy stripping and the single-scattering and OPE triangle diagrams (see Fig. 10). The expressions for the matrix ele-

ments of these processes constitute a generalization of the formulas of Sec. 4 for elastic scattering to take into account the contribution of the excited clusters as well. Thus, for the heavy-stripping mechanism we have

$$T^{p\alpha'\to p\alpha} = \binom{4}{3} \sum_{\omega\omega' t} \langle \psi_{\alpha'} | \psi_t \chi_p;\ \psi_{\omega'} \rangle \langle \psi_\alpha | \psi_t \chi_p;$$
$$\psi_\omega \rangle\, I_{\omega'\omega}(\mathbf{q}'_{pt},\ \mathbf{q}_{pt}), \qquad (31)$$

where

$$I_{\omega'\omega} = -(\varepsilon_\alpha + q'^2_{pt}/2\mu_{pt})\, \psi_{\omega'}(\mathbf{q}'_{pt})\, \psi_\omega(\mathbf{q}_{pt}). \qquad (32)$$

Here, $\langle \psi_{\alpha'} | \psi_t \chi_{p'}, \psi_{\omega'} \rangle$ and $\langle \psi_\alpha | \psi_t \chi_p, \psi_\omega \rangle$ are the single-particle structure factors for the $\langle 4N \rangle$ cluster and α particle, respectively[29]; ε_α and μ_α are the binding energy and reduced mass in the channel $\alpha \to t + p$. The wave functions $\psi_{\omega'}(q'_{pt})$ and $\psi_\omega(q_{pt})$ describe the momentum distributions at the vertices $\langle 4N \rangle \to t + p$ and $\alpha \to t + p$. At the same time, $\omega' = N_{\alpha'} L_{\alpha'} M_{\alpha'}$, $\omega = N_\alpha L_\alpha M_\alpha = 000$. For the moduli of the relative momenta $\mathbf{q}'_{pt}$ and $\mathbf{q}_{pt}$ we use the Lorentz-invariant form (18).

The matrix element of the process (30) in the framework of the single- scattering mechanism is described by Eq. (31), in which the factor $I_{\omega'\omega}$ is replaced by the expression

$$W_{\omega'\omega}(\Delta) = (2\pi)^{-3}\, T^{pp} \int d^3\rho \exp\left\{ i \frac{3}{4} \Delta\rho \right\} \psi_{\omega'}(\rho)\, \psi^*_\omega(\rho), \qquad (33)$$

where $\Delta\mathbf{k}'_N - \mathbf{k}_p$ is the momentum transfer; the wave functions $\psi_{\omega'}(\boldsymbol{\rho})$ and $\psi_\omega(\boldsymbol{\rho})$ are related to the functions $\psi_{\omega'}(\mathbf{q}'_{pt})$ and $\psi_\omega(\mathbf{q}_{pt})$ from (32) by an inverse Fourier transformation; T^{pp} is the t matrix of elastic pp scattering.

For the OPE mechanism, the cross section of the $(p, p\alpha)$ reaction can be expressed in terms of the cross section of the $pt \to \alpha\pi$ process.[73] A dependence of the spatial part of the $\langle 4N \rangle$-cluster function is contained in the integral

$$\mathcal{F}_{N_{\alpha'} L_{\alpha'} L}(Q,\ \varkappa) = \int_0^\infty d\rho j_L(Q\rho)(\varkappa\rho + 1) \exp(-\varkappa\rho)\, R_{N_{\alpha'} L_{\alpha'}}(\rho), \qquad (34)$$

where $R_{N_{\alpha'} L_{\alpha'}}(\rho)$ is the radial part of the wave function $\psi_{\omega'}(\boldsymbol{\rho})$ for the state with orbital angular momentum $L_{\alpha'}$ in the channel $\langle 4N \rangle \to t + p$; j_L is a spherical Bessel function of order $L (L = L_{\alpha'} \pm 1)$; and $\varkappa$ and Q are defined in the same way as in Refs. 44 and 45. In the calculations, we shall use the differential cross sections of the $pt \to \alpha\pi$ and pp scattering processes obtained on the basis of the procedure explained in Refs. 61 and 64. Bearing in mind that the main component of the wave function of a free α particle in the TISM has the form

$$|\psi_\alpha\rangle = |N_\alpha = 0\ [4]\ (00)\ L_\alpha = 0\ S_\alpha = 0\ T_\alpha = 0\ J_\alpha = 0\rangle, \qquad (35)$$

we find in accordance with the selection rules at the vertex $t + p \to \alpha$ for the heavy-stripping and single-scattering diagrams that the internal state of the $\langle 3N \rangle$ cluster is fixed and that the fragment t has the quantum numbers of the free triton,

$$|\psi_t\rangle = \left| N_t = 0\,[3]\,(00)\, L_t = 0\, S_t = \tfrac{1}{2}\, T_t = \tfrac{1}{2}\, J_t = \tfrac{1}{2} \right\rangle, \qquad (36)$$

and the summation over t in Eq. (31) applies only to the spin–isospin projections. The OPE diagram allows for the $\langle 3N \rangle$ fragment both the ground state (36) and excited states, but the contribution of the latter can be ignored here. The point is that in the framework of the mechanisms known in the literature[86] and used to describe the $pt \to \alpha\pi$ reaction in the region of energies 300–600 MeV at large momentum transfer the transition with $L = 0$ is dominant. Further, proceeding from the expression (36), we find in accordance with the TISM selection rules for the vertex $\langle 4N \rangle \to t + p$ that for all the considered mechanisms of the process (30) two values of the Young diagram of the cluster wave function $[f_{\alpha'}]$ are allowed, namely, [4] and [31]. As a result, for a $1p$-shell target nucleus we have the following values of the quantum numbers α' over which the summation is made in the expression (31):

$$[f_{\alpha'}] = [4],\ S_{\alpha'}\ T_{\alpha'} = 00\ N_{\alpha'} = 0,\ 1,\ 2,\ 3,\ 4; \qquad (37)$$

$$[f_{\alpha'}] = [31],\ S_{\alpha'}\ T_{\alpha'} = 10,\ 01,\ 11,\ N_{\alpha'} = 1,\ 2,\ 3. \qquad (38)$$

At the same time, $(\Lambda_{\alpha'} \mu_{\alpha'}) = (N_{\alpha'} 0)$, and the orbital angular momentum $L_{\alpha'}$ is determined by the following conditions: $L_{\alpha'} \leqslant N_{\alpha'}$, $L_{\alpha'} + N_{\alpha'}$ is an even number.

For the function $\psi_\omega(\rho)$ in Eqs. (32) and (33) we use the Eckart parametrization,[57] which agrees with the charge form factor of the α particle in a wide range of momentum transfers and has the correct asymptotic behavior. The function $\psi_{\omega'}$ is the product of the oscillator function $\psi_{NLM}(\rho)$ and the correlation factor (13) and is normalized to unity.

Results of calculations of the characteristics of the $(p, p\alpha)$, $(p, p^3\mathrm{He})$, and $(p, p^3\mathrm{H})$ reactions for the target nucleus ^{12}C

We give below the results of our calculations of the characteristics of reactions of quasielastic knockout from the ^{12}C nucleus of protons with energy 665 MeV by fast ^{3,4}He and ^{3}H nuclei at angle 5.5° to the direction of the incident beam. The choice of these values of the energy and angle, and also the target, is due to the possibility of comparison with experimental data obtained at Dubna.[10,87] In addition, the ^{12}C nucleus can be comparatively well described by the shell model, and we had already calculated all the structure factors needed here.[26,27]

To calculate the excitation spectra of the residual nuclei it is necessary to know the positions of their levels E_f and the natural widths γ_f. Detailed information about these quantities is available only for states with the s^4p^{A-4} configuration.[24,88] In the case of states with a broken s shell the situation is much more complicated; as a rule, the experiments reveal entire groups of levels characterized by large values of γ_f, and corresponding calculations for them are lacking. Here, as usual, to describe transitions to states of nuclei with the s^4p^{A-4} configuration we use intermediate coupling both for the target nucleus and for the residual nucleus. The levels of nuclei with a broken s shell are treated in pure LS coupling; this evidently somewhat overestimates the contribution of the transitions to these states. However, the construction of an intermediate-coupling model for such states and its use in actual calculations at the present computational level does not seem possible. The mean position and width of a group of levels with one hole in the s shell were chosen in accordance with the data on the $(p, 2p)$ and (e, ep) reac-

tions[89]: $E_f = 20$ MeV, $\gamma_f = 15$ MeV for the s^3p^6 configuration and, respectively, 16 MeV and 10 MeV for the s^3p^5 configuration; for the two-hole states we used data on the (π, NN) reaction[90]: 35 MeV and 20 MeV for the s^2p^7 configuration and 32 MeV and 15 MeV for the s^2p^6 configuration. For the three- and four-hole states the analogous data are lacking. In this case, the values of E_f and γ_f were chosen by linear extrapolation of the corresponding values for the states with one and two holes: $E_f = 50$ MeV, $\gamma_f = 25$ MeV for s^1p^8, 48 MeV and 20 MeV for s^1p^7, and 64 MeV and 25 MeV for the s^0p^8 configuration, respectively.

a) Results for the heavy-stripping mechanism

Figures 11 and 12 show the angular correlation function, and Fig. 13 shows the energy distributions of the secondary protons for the (p, p^4He) reaction. The results of the calculations for the (p, p^3H) and (p, p^3He) reactions are similar.[73] The calculations of the angular correlation function in the plane-wave approximation demonstrate all the features. First, the contribution of excited clusters is appreciable and comparable with the contribution of the ground state $N_{x'} = 0$, the only exception being the states with number of quanta equal to $N_{x'} = 1$, the contribution of which is strongly suppressed by features of the structure.[4)]

Second, there is destructive interference of the amplitudes corresponding to the transitions with $N_{x'} = 0$ and to the sum over $N_{x'} \neq 0$. Because of these factors, the result obtained when allowance is made for all states of the clusters differs appreciably from the result predicted in the usual approach; instead of the maximum at the point $k_B = 0$ expected when allowance is made for only the ground state with $N_{x'} = 0$ a minimum is observed. These conclusions still remain valid when the distortions are taken into account.

The part played by the distortions in the entrance and exit channels of the $A(p, px)B$ reactions, and also in the elementary process $px' \to px$, is demonstrated in Fig. 12. It can be seen that allowance for the distortions leads to a decrease by one or two orders of magnitude in the value of the quasielastic knockout cross section but hardly changes the shape of the angular correlation function. This conclusion also extends to the energy distributions of the secondary protons (Fig. 13).

The weak sensitivity of these characteristics to allowance for the distortions is due to the high energies of the relative motion in all the reaction channels. As follows from

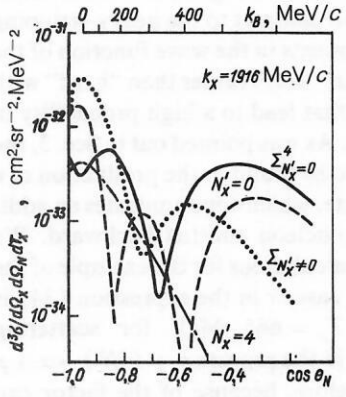

FIG. 11. Angular correlation function in the reaction ^{12}C(p, p^4He)^{8}Be (ground state) in the plane-wave approximation.

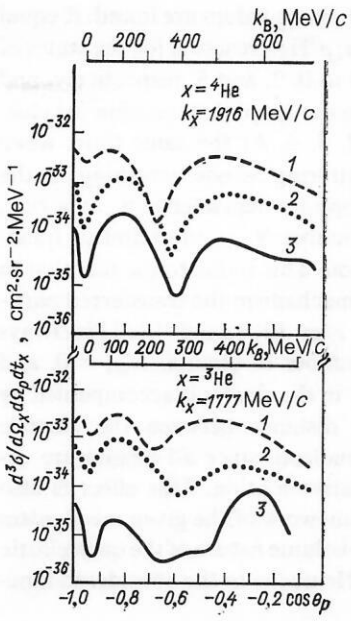

FIG. 12. Angular correlation function in the reactions ^{12}C(p, p^3He)^{9}Be (ground state) and ^{12}C(p, p^4He)^{8}Be (ground state): (1) plane waves; (2) allowance for distortions of the momentum distribution $\varphi_{N\Lambda M\Lambda}(\mathbf{k}_B)$; (3) complete allowance for distortions (distortions of the momentum distribution plus rescattering in the quasifree process).

the qualitative analysis made in Secs. 1 and 2, the influence of the distortions on the excited and unexcited clusters is different, the contribution of the excited clusters being suppressed more strongly by the distortions of the plane waves than is the case for the unexcited clusters. The calculations show that this effect does indeed occur, but under the considered kinematic conditions its magnitude is small. Let us consider, for example, the ratios of the differential cross sections calculated, respectively, in the plane-wave approximation and with allowance for the distortions of the momentum distribution $\Phi_{\nu\Lambda}$ in the most important region of the principal maxima:

$$R = (d^3\sigma/d\Omega_x\, d\Omega_p\, dE_x)^{\text{plane}}_{\max} / (d^3\sigma/d\Omega_x\, d\Omega_p\, dE_x)^{\text{dist}}_{\max}\ .$$

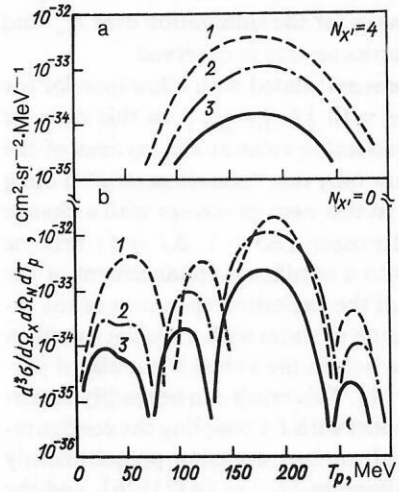

FIG. 13. Energy distribution of secondary protons in the reaction ^{12}C(p, p^4He)^{8}Be (ground state): (1) plane waves; (2) with allowance for distortions of the momentum distribution $\varphi_{N\Lambda M\Lambda}(\mathbf{k}_B)$; (3) complete allowance for distortions.

For these quantities, the following values are found: R equal to 3.3, 6.0, and 6.0 in the $(p, p^3\mathrm{He})$ reaction for the states of the clusters with $N_{x'}$ equal to 0, 2, and 3, respectively, and $R = 1.3$, 2.0, 3.8, and 3.8 in the $(p, p^4\mathrm{He})$ reaction for clusters with N_x equal to 0, 2, 3, 4. At the same time, when allowance is made for rescattering (elastic screening) in the elementary process, the opposite dependence is, as a rule, observed—the larger the number N_{x-1} of excitation quanta, the weaker the absorption. This is due to the fact that in the framework of the pole mechanism the transferred particle $x - 1$ [see, for example, Figs. 10(b) and 10(c)] is always characterized by a zero number of quanta, $N_{x-1} = 0$, and therefore an increase of $N_{x'}$ in the cluster is accompanied by an increase in the mean distance between the particle $(x - 1)$ and the emitted nucleon, since all quanta are expended solely on their relative motion. This effect is also small. Therefore, in the framework of the given mechanism one can basically speak of a volume nature of the quasielastic knockout of the ^{3}H and ^{3,4}He nuclei in the considered kinematic region.

Excited clusters can be most clearly manifested in the excitation spectrum of the residual nucleus. This is due to the fact that for the principal component of the target-nucleus wave function with zero quantum numbers $L_A = 0$, $S_A = 0$, $T_A = 0$ and $[f_A] = [444]$ in the impulse approximation the residual nucleus "remembers" the quantum numbers of the cluster with which it, the cluster, was characterized at the time of interaction with the incident proton, i.e., $T_{x'} = T_B$, $S_{x'} = S_B$, and $[f_{x'}] \times [f_B] \to [444]$.

Figure 14 shows the calculated excitation spectrum of the ^{8}Be nucleus in the $(p, p^4\mathrm{He})$ reaction (the experimental resolution was taken to be 2 MeV). We mention the two most important features of the results. The first of them is associated with the allowance for excited clusters with different values of $N_{x'}$ and $L_{x'}$ within one symmetry Young diagram $[f_x] = [f_{x'}] = [4]$ (transitions diagonal with respect to $[f_x]$). Allowance for all possible diagonal transitions in the quasifree process $px' \to px$ leads to a decrease of the cross section because of destructive interference of the amplitudes corresponding to clusters with $N_{x'} = 0$ and to the sum over $N_{x'} \neq 0$. For comparison, we note that in the framework of the diffraction theory of multiple scattering, in which $[f_{x'}] = [f_x]$ always for the summation over $N_{x'}$ and $L_{x'}$, an increase of the cross section is observed.[17]

The second feature is associated with allowance for the nondiagonal transitions with $[f_{x'}] \neq [f_x]$; in this case for $[f_x] = [4]$ the TISM selection rules at the vertices of the diagram in Fig. 10a allow only one "nonsymmetric" Young diagram $[f_{x'}] = [31]$. In this case, processes with a change of the cluster spin and isospin ($\Delta S = 1$, $\Delta T = 1$) become possible, and this leads to a significant enhancement of the spin–isospin structure of the excitation spectrum of the residual nucleus in the region of states with a broken s shell. A group of levels with one hole in the s shell is populated particularly strongly (Fig. 14). This result can be readily understood; for in the shell model with LS coupling the configuration s^3p^5 of the residual nucleus contains predominantly states with the Young diagram $[f_B] = [432][26]$, and the formation of them for the main component of the ^{12}C wave function (see above) is possible in accordance with the selection rules for Young diagrams [1] only when there is separation of clusters with a nonsymmetric diagram [31]: $[444] \to [431] \times [31]$. As a result, owing to the contribution of the clusters with the Young diagram [31], the main maximum of the total curve, which is situated at $E^* = 0$ when no allowance is made for the excited clusters, is shifted to the region of residual-nucleus states with a broken s shell and is increased in value by five times.

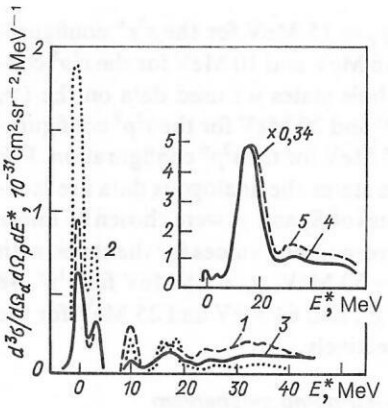

FIG. 14. Excitation spectrum of the ^{8}Be nucleus in the reaction ^{12}C$(p, p^4\mathrm{He})^8$Be with allowance for the distortions of the momentum distribution $\varphi_{N\Lambda M\Lambda}(\mathbf{k}_B)$: (1) $[f_{x'}] = [4]$, $N_{x'} = 0$; (2) $[f_{x'}] = [4]$, sum over $N_{x'} \neq 0$; (3) $[f_{x'}] = [4]$, sum over all $N_{x'}$; (4) total result with allowance for all states for $[f_{x'}] = [4]$ and $[f_{x'}] = [31]$; (5) total result without allowance for distortions (multiplied by a factor 0.34).

In the $(p, p^3\mathrm{H})$ and $(p, p^3\mathrm{He})$ reactions, the contributions of the transitions diagonal, $[f_{x'}] = [3]$, and nondiagonal, $[f_{x'}] = [21]$, with respect to the Young diagram are characterized by analogous properties.[73]

Why is the contribution of the excited clusters so large in the framework of the heavy-stripping mechanism? The reason for this is that the heavy-stripping mechanism distinguishes the high-momentum component in the wave function of the knocked-out cluster. Thus, in the kinematic region that we have considered for the $(p, p^4\mathrm{He})$ reaction the relative momentum q'_{pt} in the $\alpha \to t + p$ channel is in the region 2.5–3.4 F^{-1}. When either the initial energy or the proton scattering angle is reduced, the momentum q'_{pt} is decreased, and with it the contribution of the de-excitation processes.[73]

b) Other mechanisms of elementary processes

There is a quite different picture of quasielastic knockout when the OPE mechanism is used to describe the elementary process. To a considerable degree, this is due to the fact that in the given case, in contrast to the heavy-stripping mechanism, it is the components in the wave function of the knocked-out particle that are "soft" rather than "hard" with respect to the momentum that lead to a high probability of knockout of fast fragments. As was pointed out in Sec. 3, the physical reason for this is to be found in the production of a pion in the intermediate state, which communicates an additional momentum to the nucleon emitted backward. We consider the results of the calculations for the example of the $(p, p^4\mathrm{He})$ reaction. In this case, $\varkappa$ in the expression (34) is fairly large—at energy $T_p = 665$ MeV for scattering through angle $\theta_{\mathrm{cms}} = 180°$ in the process $p + \langle 4N \rangle \to \alpha + p$ we have $\varkappa = 1$ F^{-1}. Therefore, because of the factor $\exp(-\varkappa\rho)$ the integral $\mathcal{F}_{N_{\alpha'}L_{\alpha'}L}(Q, \varkappa)$ is small for functions

$R_{N_{\alpha'}L_{\alpha'}}(\rho)$ that vanish at the point $\rho = 0$, i.e., for states with $L_{\alpha'} \neq 0$. As a result, transitions with $L_{\alpha'} = 0$ are dominant. In addition, the contribution of the states $N_{\alpha'}L_{\alpha'} = 40$ and 20 is reduced somewhat by virtue of the single-particle structure factors.[29] Transitions with a change in the spin $S_{\alpha'}$ and isospin $T_{\alpha'}$ of a cluster are also suppressed because the Young diagram $[f_{\alpha'}] = [31]$, which allows $S_{\alpha'} = 1$ and $T_{\alpha'} = 1$, is not compatible with the state $N_{\alpha'}L_{\alpha'} = 00$ [see (38)]. The upshot is that the characteristics of the QKNC reaction are changed little when allowance is made for the excited clusters (Figs. 15 and 16).

Similar results (but for a different physical reason) are obtained when the single-scattering mechanism is used. In this case, in the region of momentum transfers $\Delta = 8$–$10\ F^{-1}$, we require particularly high-momentum components in the wave function; these cannot be ensured by the average nuclear field alone and are generated exclusively by the short-range NN correlations. The influence of these is most important in the states of clusters with $L_{\alpha'} = 0$ (see below). Therefore, the contribution of clusters with $N_{\alpha'}L_{\alpha'}$ equal to 00, 20, 40 is the most important one for the single-scattering mechanism. Formally, this is manifested in the fact that at $\Delta = 8$–$10\ F^{-1}$ the integrand in the expression (33) oscillates strongly with respect to ρ on account of the factor $\exp(i\frac{3}{4}\Delta\rho)$, and the main contribution to the integral is made by the region $\rho \sim 0$, in which the functions with $L_{\alpha'} \neq 0$ die out rapidly. At the same time, in the region of smaller momentum transfers, $\Delta \sim 2.5$–$3.5\ F^{-1}$, corresponding to slow α particles in the final state, $T_\alpha = 30$–60 MeV, the analysis shows that for the single-scattering mechanism the contribution of the excited clusters with $N_{\alpha'}L_{\alpha'} \neq 00$ in the amplitude of the $p + \langle 4N \rangle \to p + \alpha$ process is dominant by more than an order of magnitude compared with the ground state.

We note that although the contribution of the excited clusters for the OPE and single-scattering mechanisms is appreciably less than the contribution of the ground state, allowance for them does enhance the intensity of the transitions both to the ground state and to the excited states by 1.5–2 times. This is due to the strong interference of the transition amplitudes for the ground state with the total amplitude for the excited states corresponding to the Young diagram $[f_{\alpha'}] = [4]$. And whereas the heavy-stripping

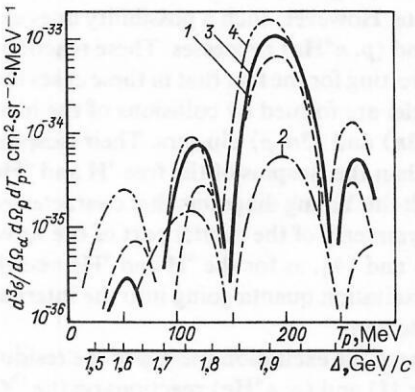

FIG. 15. Energy distribution T_p of secondary protons in the reaction $^{12}C(p, p^4He)^8Be$ (ground state) for the one-pion exchange mechanism in the plane-wave approximation: (1) $[f_{x'}] = [4]$, $N_{x'} = 0$; (2) contribution of all transitions apart from $[f_{x'}] = [4]$, $N_{x'} = 0$; (3) total result; (4) total result for the single-scattering mechanism. The momentum transfer Δ is plotted in the lower scale.

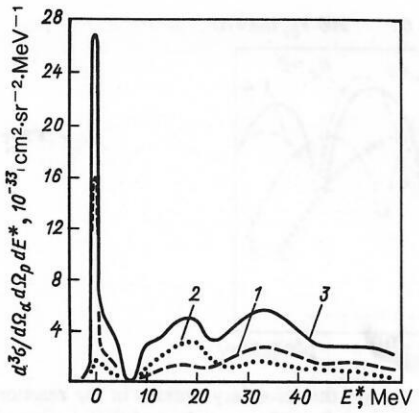

FIG. 16. Excitation spectrum of the ^8Be nucleus in the reaction $^{12}C(p, p^4He)^8Be$ for the one-pion exchange mechanism: (1) $[f_{x'}] = [4]$, $N_{x'} = 0$; (2) contribution of all transitions except for $N_{x'} = 0$; (3) total result.

mechanism predicts a destructive nature of this interference in the region of the principal maxima, both the OPE and single-scattering triangle diagrams lead to constructive interference.

In this paper, we have not considered the interference of the heavy-stripping, OPE, and single-scattering mechanisms for the reasons indicated in Sec. 4. In addition, as direct calculations of the dynamical factors I_{NLM}, W_{NLM}, and $\mathcal{F}_{NLL'}$ for the (p, p^4He) reaction show,[73] the heavy-stripping amplitude exceeds by an order of magnitude the corresponding OPE and single-scattering amplitudes in the considered kinematic region for all excited clusters. For the ground state $N_{\alpha'} = 0$, as for free $p\alpha$ backward scattering,[61] the heavy-stripping mechanism is also dominant in the quasifree process (30) in the region of initial energies 600–800 MeV. For example, in the region $k_B < 400$ MeV/c the factor $|I_{000}|$ exceeds $|W_{000}|$ by 3–4 times. The total result for the cross section obtained with allowance for all states of the excited clusters in the framework of the heavy-stripping mechanism exceeds by 4–5 times the cross sections predicted by the OPE and single-scattering mechanisms.

Influence of short-range correlations on the characteristics of QKNC reactions

The description of the association of nucleons in the framework of the TISM corresponds to allowance for the long-range correlations due to the existence of an average nuclear field and the Pauli principle. Besides the long-range correlations in the internal state of the association the repulsion at short relative distances is taken into account explicitly. Allowance for the short-range correlations under certain assumptions[42] reduces to multiplication of the wave function of the relative motion in the channel $x' \to (x-1) + N$ by the factor (13), whose form and parameters are taken to be the same for the ground and excited states of the clusters.

All the presented results were obtained with allowance for short-range NN correlations. In order to establish the extent to which the contribution of the excited states of the clusters can influence the possibility of extracting information about the short-range correlations from QKNC reactions, we made additional calculations in which we compared for the heavy-stripping mechanism the energy

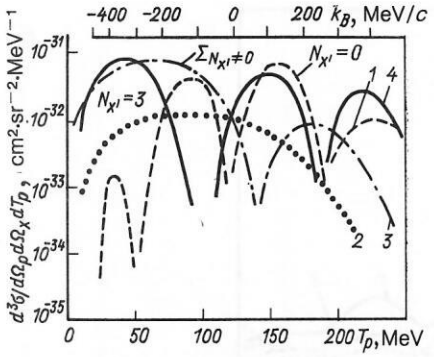

FIG. 17. Energy distribution of the secondary protons in the reaction $^{12}C(p, p^3He)^9Be$ (ground state) for different values of the number of oscillator excitation quanta $N_{x'}$ of the knocked-out association with allowance for short-range correlations: (1) $N_{x'}=0$; (2) $N_{x'}=3$; (3) contribution of only the excited clusters with $N_{x'}\neq 0$; (4) total result.

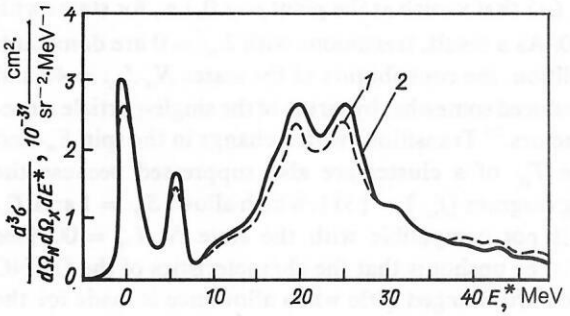

FIG. 18. Excitation spectrum of the residual nucleus without allowance (1) and with allowance (2) for the short-range correlations for the reaction $^{12}C(p, p^3He)^9Be$ at $T_0 = 450$ MeV.

distributions of the secondary protons and the excitation spectra of the residual nuclei with and without allowance for the short-range correlations.

The results of the calculation of the energy distributions of the secondary protons in the reaction $^{12}C(p, p^3He)^9Be$ (ground state)[42] show, as expected, that without allowance for the short-range correlations the contribution of the excited clusters with greater enhancement of high-momentum components to the cross section exceeds the contribution of the ground state by 3–4 orders of magnitude, the enhancement being stronger, the larger $N_{x'}$. Because of this, without allowance for the short-range correlations the main contribution to the cross section is made by clusters formed from 1p-shell nucleons. As can be seen from Fig. 17, allowance for the short-range correlations increases the contribution of the clusters with $N_{x'}=0$ by several orders of magnitude. Thus, the large momentum transfer in the case of knockout of clusters in the ground states of the internal motion is realized predominantly through the repulsion at short distances of the nucleons that form the clusters. With regard to the excited clusters, their contribution is also increased, but less significantly, and by a smaller amount, the larger is $N_{x'}$. As a result, at initial energy $T_p = 665$ MeV for transitions to states of the residual nucleus with an unbroken s shell there is an approximate equalization of the contributions of clusters with different $N_{x'}$, and this leads to an abrupt change in the shape of the total curves. Since in transitions to states of the residual nuclei with a broken s shell it is mainly clusters with $N_{x'}=0$ that participate, allowance for the short-range correlations leads to an appreciable growth in the intensity of such transitions.

Overall, the cross sections of the considered reactions increase when the short-range correlations are taken into account in the framework of the heavy-stripping mechanism. A particularly strong growth (by 2–3 orders of magnitude) is predicted for the (p, p^4He) reaction. In the reactions with $\langle 3N\rangle$ clusters, the increase in the cross section is not so pronounced. Moreover, as can be seen from the calculations in Fig. 18, for smaller values of the incident protons ($T_p = 450$ MeV, $q\sim 7$ F^{-1}) the amplitude for scattering by an excited cluster in the (p, p^3H) reaction becomes insensitive to the allowance for the short-range correlations. And although the contribution of the ground state increases by two orders of magnitude while the contribution of the excited clusters remain practically unchanged, the transitions on excited clusters are still dominant, and the total cross section is hardly changed in this case (Fig. 18) when the short-range correlations are taken into account.

Thus, because of processes with de-excitation of the clusters, the long-range shell correlations can play an important part in the region of large momentum transfers in QKNC reactions.

In the framework of the OPE mechanism, allowance for the short-range correlations leads not to an increase but, instead, to a decrease in the knockout probability, since the correlation factor (13) reduces the wave function $\psi_{N_x L_x M_x}(\rho)$ in the neighborhood of the point $\rho = 0$. The calculations show that this effect is small, the contribution of the states with $L_{x'}=0$ being decreased by only 1.2–4 times, while the contribution of the states with $L_{x'}\neq 0$ is practically unchanged.

Thus, the quantitative and even qualitative manifestation of the short-range correlations depends strongly on the mechanism of the quasifree process $px'\to px$.

Possibility of the formation of fast ^{3}H and ^{4}He nuclei in the (p, n^3H) and (p, n^4He) reactions on the ^{12}C nucleus

The investigations made above into the part played by processes with rearrangement of the internal states of knocked-out particles in QKNC reactions showed that the contributions of the ground state and the excited states of the clusters overlap strongly, as a rule, and this seriously reduces the possibility of identifying transitions in which only excited clusters participate. However, such a possibility does exist in the (p, n^3H) and (p, n^4He) processes. These reactions are particularly interesting for the fact that in these cases the fast ^{3}H and ^{4}He nuclei are formed by collisions of the incident protons with $\langle 3n\rangle$ and $\langle 3n, p\rangle$ clusters. Their isospins are larger by unity than the isospins of the free ^{3}H and ^{4}He nuclei, and as a result the Young diagrams that characterize the permutational symmetry of the orbital part of the wave function are not [3] and [4], as for the ^{3}H and ^{4}He nuclei, and the number of excitation quanta going into the internal motion is not equal to zero.

We have calculated the excitation spectra of the residual nuclei for the (p, n^3H) and (p, n^4He) reactions on the ^{12}C nucleus for the same kinematic conditions as for the (p, p^3H) and (p, p^4He) reactions considered earlier. Most of the calculations were made in the framework of the heavy-stripping mechanism. We determine the states of the clusters x' that are possible in the TISM and that must be taken into account

in the given case. Since the $\langle 3n\rangle$ cluster has isospin 3/2, the two Young diagrams [21] and [111] are allowed, though the latter does not contribute to the matrix element of the process. Therefore, only the single spin value $S_{x'} = 1/2$ is allowed. The possible values of $N_{x'}$ and $L_{x'}$, and also of the Elliott symbols $(\lambda_{x'}\mu_{x'})$, can be found from the tables for the corresponding cluster coefficients[26]: $N_{x'}L_{x'}$ $(\lambda_{x'}\mu_{x'}) = 20$ (20), 22 (20), and 11 (10). Note that in this case for a 1p-shell target nucleus the minimal, $N_{x'} = 0$, and maximal, $N_{x'} = 3$, numbers of quanta do not contribute to the cross section. The first of them is not compatible with the Young diagram [21], and the second is not compatible with the condition $(\lambda_{x'}\mu_{x'}) = (N_{x'}0)$, which follows from the selection rules for the Elliott symbols in the case of the heavy-stripping mechanism.[74]

One can show similarly that a contribution to the matrix element of the $(p, n^4\mathrm{He})$ reaction is made by the following states of the $\langle 3n, p\rangle$ clusters: $[f_{x'}] = [31]$, $T_{x'} = 1$, $S_{x'} = 0$ and 1, $(\lambda_{x'}\mu_{x'}) = (N_{x'}0)$, $N_{x'}L_{x'}$ equal to 11, 20, 22, 31, 33.[26]

The results of the calculations are given in Figs. 19, 20, and 21, and also in Table I, in which we introduce the integrated cross section S, which is defined by the equation

$$S(p,\ Nx) = \int_A^B dE^* \frac{d^3\sigma}{d\Omega_x\, d\Omega_N\, dE^*}\ , \qquad (39)$$

where $A = 8$ MeV and $B = 60$ MeV.

Analysis of the data permit the following conclusions to be drawn[91]:

(a) the cross sections of the $(p, n^3\mathrm{H})$ and $(p, n^4\mathrm{He})$ reactions are comparable with those of the $(p, p^3\mathrm{H})$ and $(p, p^4\mathrm{He})$ reactions in the corresponding regions of excitation energy of the residual nucleus. This conclusion is practically independent of the experimental resolution ΔE.

(b) The $(p, n^3\mathrm{H})$ and $(p, n^4\mathrm{He})$ reactions are realized primarily through transitions to the states of the residual nucleus with one hole in the s shell (Figs. 20 and 21). This is due to the structure of the s^3p^6 and s^3p^5 hole levels; for in the shell model with LS coupling these configurations correspond to a large number of states with the Young diagrams [432] and [431] (Ref. 26), which, when multiplied with the Young diagrams [21] and [31], respectively, contain the Young diagram [444] of the main component of the target-nucleus wave function.

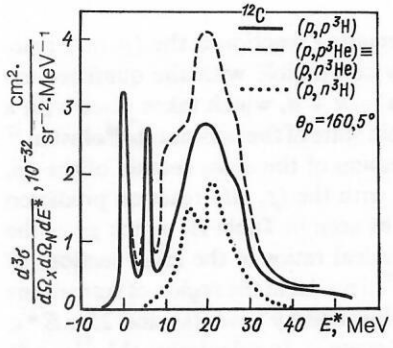

FIG. 19. Excitation spectra of residual nuclei in the reactions of quasielastic knockout of ^{3}H and ^{3}He nuclei with allowance for all possible states of the knocked-out $\langle 3N\rangle$ clusters. The calculation was made with allowance for the distortions of the momentum distribution $\varphi_{N\Lambda M\Lambda}(\mathbf{k}_B)$.

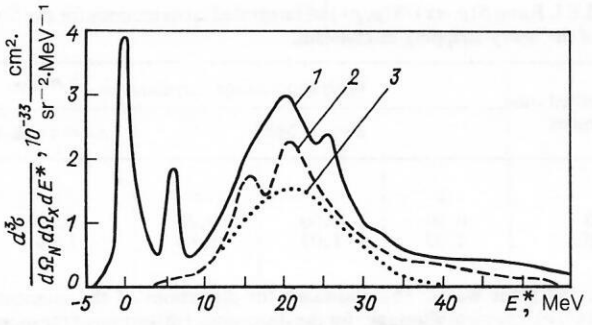

FIG. 20. Excitation spectra of residual nuclei in $^{12}\mathrm{C}(p, N^3\mathrm{H})$ reactions with complete allowance for distortions: (1) $N = p$; (2) $N = n$; (3) $N = n$, contribution of transitions to states with configuration s^3p^{A-3-x}.

(c) Allowance for the short-range correlations changes the ratio of the cross sections only slightly (Table I).

We note that when the OPE mechanism is used to describe the elementary process $px' \to Nx$ the $S(p, nx)/S(p, px)$ cross-section ratio is reduced by about an order of magnitude. This comes about because of the decrease in the relative contribution of the states of excited clusters with $L_{x'} \neq 0$. A further reason for the decrease in the relative yield of neutrons is also to be found in the isotopic relations; for example, for $x = {}^4\mathrm{He}$ for the OPE mechanism we have (provided the spatial functions of the $\langle 3n, p\rangle$ cluster and the α particle are the same)

$$\sigma(p\ \langle 3n,\ p\rangle \to n\alpha)/\sigma(p\alpha \to p\alpha) = 2/9,$$

whereas for the heavy-stripping mechanism we have

$$\sigma(p\ \langle 3np\rangle \to n\alpha)/\sigma(p\alpha \to p\alpha) = 2.$$

When the single-scattering mechanism is used, the ratio $S(p, nx)/S(p, px)$ must also be less than unity, since in this case too the contribution of the transitions with $L_x \neq 0$ is significantly suppressed compared with the contribution of the ground state of the clusters.

5. COMPARISON WITH EXPERIMENT

Knockout of ^{3,4}He and ^{3}H nuclei

In this case, the experimental situation has hardly changed during the last ten years.[10,87] The recent coincidence data on reactions of the type $(p, p\alpha)$ either correspond to low energies $T_p = 100$–150 MeV,[8,9] or, at higher energies around 600 MeV, cover the region of intermediate scattering angles ($\sim 90°$ in the $p + \alpha$ center-of-mass system),[92] which has not been considered in this work.

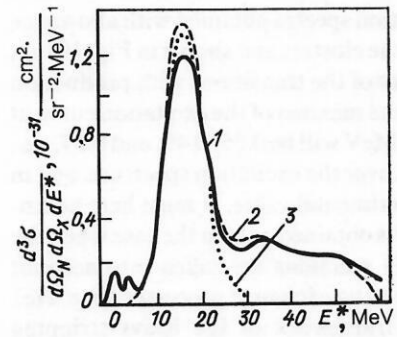

FIG. 21. Curves 1, 2, and 3 are the same as in Fig. 20 but for the reaction $^{12}\mathrm{C}(p, N^4\mathrm{He})$.

TABLE I. Ratio $S(p, nx)/S(p, px)$ of integrated cross sections for the ^{12}C nucleus in the case of the heavy-stripping mechanism.

Knocked-out fragment	With short-range correlations				Without short-range correlations
	$\Delta E = 2$ MeV			$\Delta E = 10$ MeV	
	a	b	c	b	a
^{3}H	0.80	0.50	0.71	0.52	0.98
^{4}He	1.09	1.03	1.05	1.06	0.72

Note: (a) plane waves; (b) allowance for distortions of the momentum distribution $\Phi_{\nu\Lambda}(k)$; c) complete allowance for the distortions (distortion of the momentum distribution plus rescattering in the quasifree process).

As before, from the point of view of the questions to which this review has been devoted, the experimental data on the quasielastic knockout of fast ^{3,4}He and ^{3}H nuclei[10,87] obtained in $p + A \to x + \ldots$ exclusive experiments are still the most interesting. In the work reported in Refs. 10 and 58 the energy distributions $d\sigma/d\Omega_x dE_x$ of fragments knocked out at a fixed angle were measured; the secondary nucleons and, therefore, the states of the residual nuclei were not detected. However, such integrated characteristics give only a qualitative picture of quasielastic knockout and are not sufficiently informative to establish the mechanisms of the reaction and the elementary process. The insensitivity of these characteristics to the details of the microscopic model and, in addition, the appreciable admixture of nonquasielastic processes, for which the elementary event is, for example, a reaction of the $p + (x-1) \to x + \pi$ type,[10,79,93] mean that it is not worth making lengthy calculations here of $d\sigma/d\Omega_x dE_x$. Under these conditions, it appears more sensible to compare for the time being only the ratios of the fragment-yield cross sections observed experimentally with the corresponding theoretical values.

Comparison of the energy distributions of the ^{3}H and ^{3}He nuclei from $p + {}^{12}\text{C} \to {}^3\text{H}({}^3\text{He}) + \ldots$ reactions measured in Ref. 87 in the region of the quasielastic peak (i.e., at an energy of the fragment knocked out at a definite angle corresponding to a collision of the incident proton with a cluster at rest in the target nucleus for zero excitation energy of the residual nucleus) gives a ratio 0.5 of the yields of the ^{3}H and ^{3}He nuclei. Taking into account only the ground state of the cluster, we find that in the framework of the heavy-stripping mechanism the cross sections of the $(p, p^3\text{H})$, $(p, p^3\text{He})$, and $(p, n^3\text{He})$ processes are equal to each other, while the probability of the $(p, n^3\text{H})$ process is zero, so that in this case the ratio of the ^{3}H and ^{3}He yields agrees with the experimental value 0.5. It follows from the results of calculation of the excitation spectra obtained with allowance for all possible states of the clusters and shown in Fig. 19 that the ratio of the intensities of the transitions with production of ^{3}H and ^{3}He nuclei at the maxima of the excitation curve at E^* equal to 0, 6, and 20 MeV will be 0.55, 0.49, and 0.57, i.e., approximately constant over the excitation spectrum, and in agreement with the experimental value. It must here be emphasized that this result is obtained only in the case when the $(p, p^3\text{He})$ and $(p, p^3\text{H})$ reactions are taken into account together with the quasielastic exchange processes $(p, n^3\text{He})$ and $(p, n^3\text{H})$. In the framework of the heavy-stripping mechanism, the cross sections of the $(p, p^3\text{He})$ and $(p, n^3\text{He})$ processes on the ^{12}C nucleus are equal (see Fig. 19) and on the average somewhat exceed the cross section of the $(p, p^3\text{H})$ process, while the $(p, n^3\text{H})$ reaction is characterized by a much smaller cross section than $(p, p^3\text{H})$.

Thus, the available data do not contradict the ideas which we have developed. For more definite conclusions, data from coincidence experiments are required.

Deuteron knockout

In 1979–1980, some definite progress was achieved by the carrying out at Dubna of kinematically complete experiments for the (p, pd) and (p, nd) reactions on a number of light nuclei[12,13,94] at $T_p = 670$ MeV in the region of large momentum transfers. The energy distributions of the secondary nucleons and the excitation spectra of the residual nuclei were measured. In the region of energies 600–700 MeV, as was already noted in Sec. 4, the Δ-resonance feature in the cross section of pd backward scattering has the consequence that the contribution of excited two-nucleon clusters is strongly suppressed on account of both the spatial part and the spin–isospin part of the transition amplitude. For example, as for the α-particle knockout reactions discussed in Sec. 5, the dynamical factor (34) for (p, Nd) reactions in the OPE mechanism reduces by about an order of magnitude the contribution of the transitions with nonzero internal orbital angular momentum of a pair of nucleons compared with the s states. Similarly, the isospin relations for the OPE mechanism strongly suppress transitions in which the spin–isospin structure of the clusters is changed, since in this case we have

$$\sigma(p + \langle np\rangle_{S=0,\ T=1} \to pd)/\sigma(p + \langle np\rangle_{S=1,\ T=0} \to pd) = 1/9.$$

However, for the heavy-stripping mechanism this ratio is equal to unity.

A particularly interesting reaction is the (p, nd) reaction; it is kinematically compatible with the quasifree exchange process $p + \langle 2n\rangle \to n + d$, which takes place with a change in the spin–isospin state of the two-nucleon cluster.[12] The appreciable suppression of the cross section of the (p, nd) reaction compared with the (p, pd) reaction predicted by the OPE model can be seen in Table II, which gives the experimental and theoretical ratios of the cross sections of these reactions for the ^{6,7}Li nuclei in the region of transitions $-10 \leqslant E^* \leqslant 25$ MeV ("low-energy" events) and $25 < E^* \leqslant 60$ MeV ("high-energy" events). In calculating the $\sigma(p, nd)$ to $\sigma(p, pd)$ ratio for the intensities of the excitation spectra in LS coupling, as in the calculations of the excitation spectra, we ignore transitions to states with one hole in the s shell

TABLE II. Ratio $[d\sigma(p, nd)/d\sigma(p, pd)] \cdot 10^2$ of differential cross sections.

Target nucleus	Events			
	"low-energy"		"high-energy"	
	Experiment	Theory	Experiment	Theory
^{7}Li	6,1±0,9	14,3	9,1±1,5	7,4
^{6}Li	0,30±0,16	0	8,1±1,5	6.8

in order to take into account the individuation of the α and d clusters in the ^{6}Li nucleus and the α and t clusters in Li. The low-energy events were associated with the configuration s^4p^{A-2}, and the high-energy events with the configuration s^2p^{A-4}. As can be seen from Table II, the theoretical values of the cross-section ratio in the region of two-hole excitations agree with the experimental values. However, in the region of the low-energy events for the ^{7}Li nucleus the theoretical predictions are approximately twice the experimental values. This discrepancy was partly eliminated in Ref. 34 by taking into account the difference between the NN forces in the channels with isospins $T = 0$ and $T = 1$ for a simple cluster model of the ^{7}Li nucleus.

With allowance for the distortions in the strong-absorption model, the shape and intensity of the energy distribution of the secondary protons for transitions to the ground and low-lying ($E^* < 5$ MeV) states of the residual ^{10}B nucleus in the (p, pd) reaction on the ^{12}C nucleus were obtained in Ref. 94. In the same model, the given characteristic was also reproduced in Ref. 13 for the ^{6}Li$(p, pd)^4$He reaction by means of a three-body wave function of the ^{6}Li nucleus.

We give here the results of calculations[96] of the excitation spectra of the residual nuclei in (p, pd) reactions on the ^{6}Li and ^{12}C nuclei. For ^{12}C, the energy distributions of the secondary protons have also been obtained. All calculations were made with allowance for the distortions in the strong-absorption model, and also in the eikonal approximation. For comparison, plane-wave calculations of the excitation spectra are also given.

As can be seen from Fig. 22, the energy distribution of the secondary protons in the case of transitions to low-lying states of the ^{10}B nucleus in accordance with the results of Ref. 94 is basically correct in both shape and intensity. Approximately the same results are obtained from the allowance for the distortions in both cases. However, the decrease in the absolute value of the cross sections from the plane-wave calculations needed to achieve agreement with the experiment occurs in the two cases for different reasons. In the strong-absorption model, it is a consequence of elimination of the contribution of the internal region of the nucleus, while in the eikonal approximation it comes about because of the attenuating factor $\exp(-\varkappa Rk)$ in the expression (23), which reduces the contributions from the internal and external regions equally. It is clear that this difference is manifested on the transition to the excitation spectra. It can be seen from Figs. 23 and 24 that when allowance is made for the distortions in the strong-absorption model it is possible to reproduce correctly the shape and intensity of the excitation spectra for both reactions: on ^{6}Li and on ^{12}C. Moreover, the same values of the cutoff parameters R_0 with which the

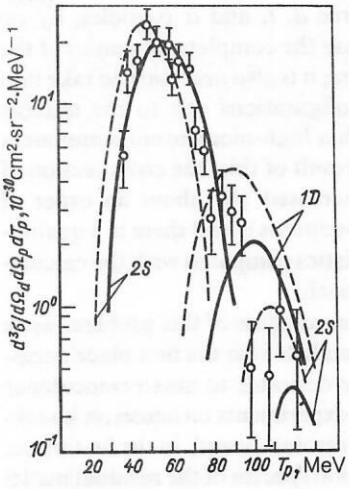

FIG. 22. Distribution with respect to the kinetic energy of the secondary protons in the reaction ^{12}C$(p, pd)^{10}$B for transitions to low-lying ($E^* < 5$ MeV) states of the residual nucleus at $T_0 = 670$ MeV, $\theta_d = 6.5°$, $\theta_p = 147°$, $\Delta E_{exp} = 17$ MeV. Calculations with allowance for distortions: the continuous curve in the strong-absorption model with $R_0 = 2.75$ F; the broken curve in the eikonal approximation with $\delta_{dB} = 0.205$, $\delta_{pA} = 0.015$, $\delta_{pB} = 0.025$, $R_{dB} = 3.78$ F, $R_{pA} = 3.94$ F, $R_{pB} = 4.18$ F, $\varkappa = 0.1\,\delta$. The dots are the data of Ref. 94. Separately given are the contributions of the $2S$ and $1D$ states of the relative motion of the deuteron in the target nucleus.

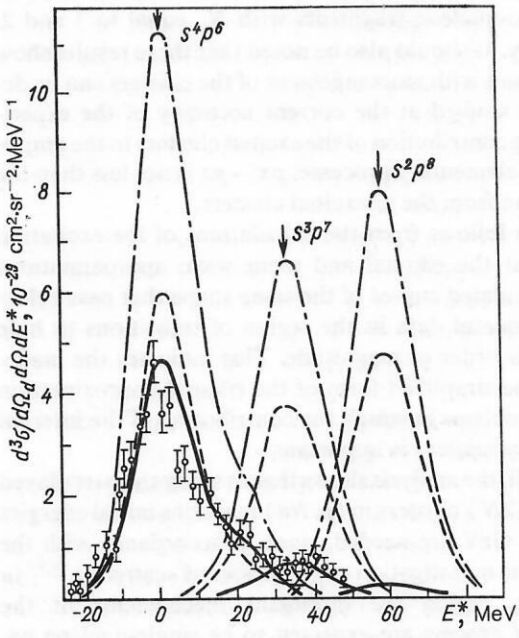

FIG. 23. Excitation spectrum of the ^{10}B nucleus in the reaction ^{12}C$(p, pd)^{10}$B; the arrows indicate the maximal contributions of the residual-nucleus configurations s^4p^6, s^3p^7, s^2p^8. The chain curve shows the plane-wave calculation, and the remaining notation is as in Fig. 22.

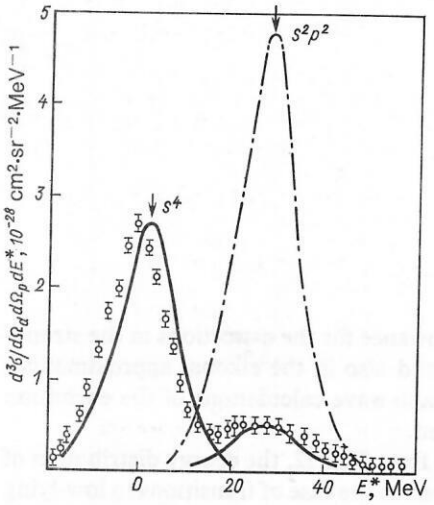

FIG. 24. Excitation spectrum of the ^{4}He nucleus in the reaction ^{6}Li(p, pd)^{4}He. The calculations: the chain curve represents the plane-wave approximation, and the continuous curve is for the strong-absorption model with $R_0 = 2.8$ F. The points are the data of Ref. 13; the arrows indicate the maximal contributions of the residual-nucleus configurations s^4 and s^2p^2.

energy distribution of the secondary protons is reproduced were used: $R_0 = 2.75$ F in the (p, pd) reaction on the ^{12}C nucleus, and $R_0 = 2.8$ F on the ^{6}Li nucleus. The allowance for the attenuation of the incident and outgoing waves in the internal region was of fundamental importance for obtaining agreement with experiment. Because of this, as can be seen from the figures, the transitions to the highly excited states of the residual nucleus with one and two holes in the s shell and with allowance for distortions are suppressed more strongly (by about an order of magnitude) than the transitions to the low-lying states with an unbroken s shell. In principle, this means that exactly the same suppression of the contribution of the light excited clusters relative to the unexcited clusters results from the distortions in the processes of quasielastic knockout with rearrangement of the excited two-nucleon fragments with N_x equal to 1 and 2, respectively. It should also be noted that these results show that processes with rearrangement of the clusters can be detected and studied at the current accuracy of the experiments if the contribution of the excited clusters to the amplitude of the elementary processes $px' \to px$ is not less than the contribution from the unexcited clusters.

It also follows from the calculations of the excitation spectra that the eikonal and plane-wave approximations lead to calculated curves of the same shape that pass below the experimental data in the region of transitions to hole states by an order of magnitude. This indicates the inadequacy of the simplified form of the eikonal approximation (23) for problems in which the contribution of the internal region of the nucleus is important.

Overall, the analysis shows that to study the part played by excited $\langle 2N \rangle$ clusters in (p, Nd) reactions initial energies $T_0 = 1$–1.5 GeV are needed, since in accordance with the results of the investigation of pd backward scattering[54,97] in this energy region the dominant mechanisms in the $p\langle 2N \rangle \to pd$ process are expected to be single-nucleon exchange (in the given case, the analog of the heavy-stripping mechanism) and single scattering. Since these mechanisms lead to equal cross sections for the singlet and triplet $\langle np \rangle$ states, transitions in which the isospin changes, $\Delta T = 1$, can, as the calculation of the ^{14}N(p, pd)^{12}C reaction[98] showed, significantly change the observed excitation spectrum of the residual nucleus.

An interesting feature is noted in the inclusive spectra of the knocked-out fast d, t, and α particles[10] in reactions on the ^{12}C and ^{16}O nuclei, and it apparently indicates a contribution of excited clusters. For deuterons, i.e., formations that are unstable and break up readily in a nucleus, a clear quasielastic peak is observed at $T_p = 670$ MeV in the process $p + A \to d + \ldots$. It is interesting that this peak is smeared in the direction of lower momenta on the transition to $T_p = 1200$ MeV.[10,99] However, for the more compact "true" clusters—the α particles—only a shoulder is observed in the region of the quasielastic maximum. Such filling of the spectral curve at secondary proton momenta less than the quasielastic maximum can be explained naturally by a large contribution of transitions to highly excited states of the residual nucleus, which, as can be seen from calculations of the excitation spectra for the (p, $p\alpha$) reaction [and is expected for the (p, pd) reaction at $T_p > 1$ GeV], are populated particularly strongly through the contribution of processes with rearrangement of excited clusters.

CONCLUSIONS

The main aim of this review was to draw the attention of the investigators to the possibility of a nontraditional interpretation of QKNC reactions based on the idea of rearrangement of the internal states of clusters in the process of their knockout from nuclei. Such an interpretation is needed if we are considering processes with large momentum transfers. Despite the large momentum transfer, when, it would appear, the knockout process must take place almost entirely through short-range NN correlations, our analysis shows that the influence of the target-nucleus structure on the reaction amplitude can be very appreciable. Indeed, allowance for the short-range correlations in only the $(0s)^3$ and $(0s)^4$ configurations, as in the free d, t, and α particles, by no means determines in this case the complete dynamics of the fast-cluster knockout process; it is also necessary to take into account the noncluster configurations due to the nuclear structure and enriched with a high-momentum component of the wave function. As a result of this, the cross section of quasielastic knockout is increased (by about an order of magnitude under certain conditions), and there is a qualitative change of the characteristics compared with the calculation in the traditional approach.

For a further and deeper analysis of this problem work on the part of the experimentalists is in the first place necessary. It would be extremely desirable to make coincidence experiments like the Dubna experiments on deuteron knockout[12,13,94] with good energy resolution and, in the first place, measurements of the excitation spectra of the residual nuclei in (p, $N\alpha$) reactions. In the theoretical field, the next stage in the development of the approach presented in this review must consist of applying such schemes for calculating nuclear structure (like the resonating-group method) in which allowance is made simultaneously for the Pauli principle and the short-range correlations. At the present time, such calculations with analytic wave functions convenient for practical use are available only for the ^{6}Li nucleus.[100]

We are very grateful to V. V. Balashov, V. I. Komarov, and V. G. Neudachin for a fruitful discussion of the questions considered here.

[1)]Of course, there is no exact correspondence between the wave function of an unexcited cluster defined in this way and the corresponding wave function of the free particle, since, for example, there are only small admixtures of the D, F, etc., components in the wave functions of the lightest nuclei.

[2)]We emphasize that any separately taken term in the expansion (5) is not antisymmetric with respect to permutation of the nucleons between the clusters x and B. It is only the sum of all terms in (5) that is antisymmetric. Therefore, if the antisymmetrization operator $\hat{A}_{Bx}$ is omitted, as is usually done,[30] then for complete allowance for the Pauli principle in the cluster nuclei $A = B + x$ it is not sufficient simply to make the ground state orthogonal to the forbidden states; instead, it is necessary to take into account in the total function of the nucleus the coupling of the channels to the excited clusters. In this way, it is possible to obtain wave functions $\psi_{\nu\Lambda}(\rho)$ with correct asymptotic behavior for both ordinary and excited clusters. The existing calculations[31] of the bound states of the ^{6}Li nucleus in the α–d model and of the ^{7}Li nucleus in the $\alpha + t$ model with Woods–Saxon potentials[30] show that the intervals between the forbidden states correspond to within a few mega-electron-volts to the energy $\hbar\omega \simeq 16$ MeV of the oscillator quantum for 1p-shell nuclei.

[3)]The existence of a surface is associated here not so much with the target nucleus (since for it there is a superposition $|A\rangle = |xB\rangle + |x^*B\rangle + \ldots$, where for each of the components there exists a corresponding rms radius between the centers of mass of the fragments x and B) as with the interaction of the initial and final reaction products with the target nucleus and the residual nucleus, respectively.

[4)]Transitions with $N_{x'} = 1$ are realized only by virtue of the small components of the nuclear functions corresponding to a lowered permutational symmetry, since the states of the three- and four-nucleon clusters with the given number of quanta are not compatible with the single-row Young diagrams $[f_{x'}] = [3]$ and $[f_{x'}] = [4]$.

[1]V. G. Neudachin and Yu. F. Smirnov, Nuklonnye assotsiatsii v legkikh yadrakh (Nucleon Associations in Light Nuclei), Nauka, Moscow (1969).

[2]D. F. Jackson, Clustering Phenomena in Nuclei, Vol. 3 (edited by K. Wildermuth and P. Kramer), Braunschweig, Vieweg (1983); P. Beregi, N. S. Zelenskaya, V. G. Neudachin, Yu. F. Smirnov *et al.*, Nucl. Phys. **66**, 513 (1965); I. Rotter and M. A. Zhusupov, Ann. Phys. (N.Y.) **17**, 57 (1966).

[3]L. S. Azhgireĭ, I. K. Vzorov, V. P. Zrelov *et al.*, Zh. Eksp. Teor. Fiz. **33**, 1185 (1957) Sov. Phys. JETP **6**, 911 (1958)].

[4]D. I. Blokhintsev, Zh. Eksp. Teor. Fiz. **33**, 1295 (1957) [Sov. Phys. JETP **6**, 995 (1958)].

[5]A. M. Baldin, Fiz. Elem. Chastits At. Yadra **8**, 429 (1977) [Sov. J. Part. Nucl. **8**, 175 (1977)].

[6]V. V. Balashov and A. N. Boyarkina, Izv. Akad. Nauk SSSR Ser. Fiz. **28**, 359 (1964); V. V. Balashov, A. N. Boyarkina, and I. Rotter, Nucl. Phys. **59**, 417 (1964).

[7]V. V. Balashov, in: Clustering Phenomena in Nuclei, IAEA, Vienna (1969), p. 59.

[8]N. S. Chant, in: AIP Conf. Proc. No. 47, Winnipeg (1978), p. 415.

[9]P. G. Roos, N. S. Chant, A. A. Cowley *et al.*, Phys. Rev. C **15**, 69 (1977); N. S. Chant, P. G. Roos, and C. W. Wang, Phys. Rev. C **17**, 8 (1978).

[10]V. I. Komarov, Fiz. Elem. Chastits At. Yadra **5**, 419 (1974) [Sov. J. Part. Nucl. **5**, 168 (1974)].

[11]L. S. Azhgireĭ, I. K. Vzorov, V. N. Zhmyrov *et al.*, Yad. Fiz. **28**, 1017 (1978) [Sov. J. Nucl. Phys. **28**, 522 (1978)].

[12]D. Albrecht, J. Erö, Z. Fodor *et al.*, Nucl. Phys. **A322**, 512 (1979).

[13]D. Albrecht, M. Csatlos, J. Erö *et al.*, Nucl. Phys. **A338**, 477 (1980).

[14]J. Arvieux, S. D. Baker, R. Beurtey *et al.*, Phys. Rev. Lett. **50**, 19 (1983).

[15]P. Berthet, R. Frascaria, B. Tatischeff *et al.*, Phys. Lett. **B106**, 465 (1981).

[16]R. H. McCamis, J. M. Cameron, L. G. Greeniaus *et al.*, Nucl. Phys. **A302**, 388 (1978).

[17]V. G. Neudachin, Yu. F. Smirnov, and N. F. Golovanova, Adv. Nucl. Phys. **11**, 1 (1979).

[18]N. S. Chant and P. G. Roos, Phys. Rev. C **15**, 57 (1977).

[19]N. Chirapatpimol, J. C. Fong, M. M. Gazzaly *et al.*, Nucl. Phys. **A264**, 379 (1976).

[20]V. V. Balashov, in: AIP Conf. Proc. No. 47, Winnipeg (1978), p. 252.

[21]N. F. Golovanova, I. M. Il'in, V. G. Neudachin *et al.*, Nucl. Phys. **A262**, 444 (1976).

[22]V. V. Balashov, V. G. Neudachin, Yu. F. Smirnov, and N. P. Yudin, Zh. Eksp. Teor. Fiz. **37**, 1385 (1959) [Sov. Phys. JETP **10**, 983 (1960)].

[23]Yu. F. Smirnov and Yu. M. Tchuvil'sky, Phys. Rev. C **15**, 84 (1977).

[24]A. N. Boyarkina, Struktura yader lp-obolochki (Structure of lp-Shell Nuclei), Moscow State University (1973).

[25]N. F. Golovanova and N. S. Zelenskaya, Yad. Fiz. **8**, 274 (1968) [Sov. J. Nucl. Phys. **8**, 158 (1969)].

[26]M. A. Zhusupov, V. I. Markov, N. A. Pyatnitsa, and Yu. N. Uzikov, Preprint 71-78 [in Russian], Institute of High Energy Physics, Kazakh Academy of Sciences, Alma-Ata (1978).

[27]M. A. Zhusupov, O. Imambekov, N. A. Pyatnitsa, and Yu. N. Uzikov, in: Prikladnaya yadernaya fizika i kosmicheskie luchi (Applied Nuclear Physics and Cosmic Rays), Kazakh State University, Alma-Ata (1979), p. 111.

[28]L. Ja. Glosman and Yu. M. Tchuvil'sky, J. Phys. C **9**, 1033 (1983).

[29]M. A. Zhusupov, V. I. Markov, and Yu. N. Uzikov, see Ref. 27, p. 93.

[30]V. G. Neudachin, V. I. Kukulin, and Yu. F. Smirnov, Fiz. Elem. Chastits At. Yadra **10**, 1236 (1979) [Sov. J. Part. Nucl. **10**, 492 (1979)].

[31]S. B. Dubovichenko and M. A. Zhusupov, Izv. Akad. Nauk Kaz. SSR Ser. Fiz.-Mat. No. 6, 25 (1983); Izv. Akad. Nauk SSSR Ser. Fiz. **48**, 935 (1984).

[32]K. Wildermuth and Y. C. Tang, A Unified Theory of the Nucleus (Academic, New York, 1977) [Russian translation published by Mir, Moscow (1980)].

[33]H. Kanada, T. Kaneko, H. Nishioko, and S. Saito, Prog. Theor. Phys. **63**, 842 (1980).

[34]H. Kanada, T. Kaneko, and Y. G. Tang, Nucl. Phys. **A 380**, 87 (1982).

[35]T. Kajino, T. Matsuse, and A. Arima, Nucl. Phys. **A414**, 185 (1984).

[36]J. M. Blatt and V. F. Weisskopf, Theoretical Nuclear Physics (Wiley, New York, 1952) [Russian translation published by Izd. Inostr. Lit., Moscow (1954)].

[37]L. Ya. Glozman, Izv. Akad. Nauk Kaz. SSR Ser. Fiz.-Mat. No. 4, 30 (1984).

[38]M. N. Braun and V. V. Vechernin, Yad. Fiz. **25**, 1276 (1977) [Sov. J. Nucl. Phys. **25**, 676 (1977)].

[39]J. L. Matthews, W. Bertozzi, M. J. Leitch *et al.*, Phys. Rev. Lett. **38**, 8 (1976).

[40]J. A. Niskanen, Nucl. Phys. **A298**, 417 (1978); L. Ya. Glosman, V. I. Kukulin, and V. G. Neudachin, Nucl. Phys. **A430**, 589 (1984).

[41]L. A. Kondratyuk, F. M. Lev, and L. V. Shevchenko, Yad. Fiz. **29**, 1081 (1979) [Sov. J. Nucl. Phys. **29**, 558 (1979)].

[42]M. A. Zhusupov, V. I. Markov, and Yu. N. Uzikov, Izv. Akad. Nauk Kaz. SSR Ser. Fiz.-Mat. No. 6, 23 (1980).

[43]B. Z. Kopeliovich and I. K. Potashnikova, Yad. Fiz. **13**, 1032 (1971) [Sov. J. Nucl. Phys. **13**, 592 (1971)].

[44]V. M. Kolybasov and N. Ya. Smorodinskaya, Yad. Fiz. **17**, 1211 (1973) [Sov. J. Nucl. Phys. **17**, 630 (1973)].

[45]L. Vegh, J. Phys. G **5**, L121 (1979).

[46]L. Veg, B. Z. Kopeliovich, and L. I. Lapidus, Pis'ma Zh. Eksp. Teor. Fiz. **32**, 481 (1980) [JETP Lett. **32**, 461 (1980)].

[47]L. A. Kondratyuk, F. M. Lev, and L. V. Shevchenko, Yad. Fiz. **33**, 1208 (1981) [Sov. J. Nucl. Phys. **33**, 642 (1981)].

[48]L. A. Kondratyuk and M. V. Terent'ev, Yad. Fiz. **31**, 1087 (1980) [Sov. J. Nucl. Phys. **31**, 561 (1980)].

[49]L. A. Kondratyuk, in: Nuklon-nuklonnye i adron-yadernye vzaimodeĭstviya pri promezhutochnykh énergiyakh. Tr. simpoziuma, 23–25 aprelya 1984 (Nucleon–Nucleon and Hadron–Nucleus Interactions at Intermediate Energies. Proc. of the Symposium, April 23–25, 1984), Leningrad (1984), p. 402.

[50]L. A. Kondratyuk and L. V. Shevchenko, Preprint ITEP No. 152, Moscow (1984).

[51]J. Arvieux, S. D. Baker, R. Beurtey *et al.*, Nucl. Phys. **A431**, 613 (1984).

[52]S. A. Gurvitz, J. P. Dedonder, and R. D. Amado, Phys. Rev. C **19**, 142 (1979).

[53]S. A. Gurvitz, Phys. Rev. C **22**, 964 (1980).

[54]S. A. Gurvitz, Phys. Rev. C **22**, 725 (1980).

[55]P. Berthet, R. Frascaria, M. P. Combes *et al.*, J. Phys. G **8**, L111 (1982).

[56]L. G. Votta, P. G. Roos, N. S. Chant, and R. Woody, Phys. Rev. C **10**, 520 (1974); V. Comparat, R. Frascaria, N. Fujiwara *et al.*, Phys. Rev. C **12**, 251 (1975).

[57]H. Lésniak, L. Lésniak, and A. Tekou, Nucl. Phys. **A267**, 503 (1976).

[58]L. C. Arnold, B. C. Clark, and R. L. Mercer, Phys. Rev. C **21**, 1899 (1980).

[59]H. S. Sherif, M. S. Abdelmonem, and R. S. Sloboda, Phys. Rev. C **27**, 2759 (1983).

[60]M. A. Zhusupov and Yu. N. Uzikov, Izv. Akad. Nauk SSSR Ser. Fiz. **46**, 2084 (1982).

[61]M. A. Zhusupov and Yu. N. Uzikov, J. Phys. G **7**, 1621 (1981).
[62]H. W. Fearing, Phys. Rev. C **16**, 313 (1977).
[63]E. Ferrari and F. Selleri, Phys. Rev. Lett. **7**, 387 (1961).
[64]G. W. Barry, Ann. Phys. (N.Y.) **73**, 482 (1972).
[65]J. Källne, H. A. Thiessen, C. L. Morris *et al.*, Phys. Rev. Lett. **40**, 378 (1978).
[66]J. M. Greben, Phys. Lett. **B115**, 363 (1982).
[67]J. R. Shepard, E. Rost, and G. R. Smith, Phys. Lett. **B89**, 13 (1979).
[68]T. Katayama, Y. Akaishi, and H. Tanaka, Prog. Theor. Phys. **67**, 236 (1982).
[69]R. G. Arnold, B. T. Chertok, S. Rock *et al.*, Phys. Rev. Lett. **40**, 1429 (1978).
[70]H. Lésniak and L. Lésniak, Acta Phys. Pol. **89**, 419 (1978).
[71]M. A. Zhusupov, Yu. N. Uzikov, and G. A. Juldasheva, in: Particles and Nuclei Tenth International Conference, Heidelberg, July 30–August 3 (1984); Book of Abstracts, Vol. 2, p. 148.
[72]F. D. Santos, A. M. Eiro, and A. Barroso, Phys. Rev. C **19**, 238 (1979).
[73]M. A. Zhusupov, V. I. Markov, and Yu. N. Uzikov, Preprint 81-09 [in Russian], Institute of High Energy Physics, Kazakh Academy of Sciences, Alma-Ata (1981).
[74]M. A. Zhusupov and Yu. N. Uzikov, Yad. Fiz. **36**, 1396 (1982) [Sov. J. Nucl. Phys. **36**, 810 (1982)].
[75]V. V. Balashov, A. N. Boyarkina, and I. Rotter, Nucl. Phys. **59**, 417 (1964).
[76]L. W. Person and P. A. Benioff, Nucl. Phys. **A187**, 401 (1972).
[77]R. I. Glauber, in: *High Energy Physics and Nuclear Structure*, edited by Alexander (North-Holland, Amsterdam, 1977); A. G. Sitenko, Fiz. Elem. Chastits At. Yadra **4**, 546 (1973) [Sov. J. Part. Nucl. **4**, 231 (1973)].
[78]B. K. Jain, Nucl. Phys. **A314**, 51 (1979).
[79]O. L. Bartaya and Dzh. V. Meboniya, Yad. Fiz. **33**, 987 (1981) [Sov. J. Nucl. Phys. **33**, 521 (1981)]; V. V. Balashov and V. I. Markov, Nucl. Phys. **A163**, 465 (1971).
[80]M. A. Zhusupov, E. Zh. Magsumov, and V. I. Markov, Phys. Lett. **B48**, 84 (1974).
[81]I. E. McCarthy and D. Pursry, Phys. Rev. **122**, 578 (1961).
[82]R. T. Janus and I. E. McCarthy, Phys. Rev. C **10**, 1041 (1974).
[83]N. S. Zelenskaya and I. B. Teplov, Obmennye protsessy v yadernykh reaktsiyakh (Exchange Processes in Nuclear Reactions), Moscow State University (1985).
[84]M. L. Goldberger and K. M. Watson, Collision Theory, Wiley, New York (1964) [Russian translation published by Mir, Moscow (1967)].
[85]D. A. C. Ciofi, Nucl. Phys. **A106**, 215 (1968).
[86]H. W. Fearing, Phys. Rev. C **11**, 1210 (1975); V. S. Ehasin, Phys. Lett. **B69**, 297 (1977); W. R. Gibbs and A. T. Hess, Phys. Lett. **B68**, 205 (1977).
[87]V. I. Komarov, G. E. Kosarev, E. S. Kuzmin *et al.*, Nucl. Phys. **A256**, 362 (1976).
[88]F. Ajzenberg-Selove, Nucl. Phys. **A320**, 1 (1979).
[89]G. Jacob and Th. A. Maris, Rev. Mod. Phys. **45**, 6 (1973).
[90]T. I. Kopaleĭshvili, Fiz. Elem. Chastits At. Yadra **2**, 441 (1971) [Sov. J. Part. Nucl. **2**, No. 2, 87 (1971)].
[91]M. A. Zhusupov, V. I. Markov, and Yu. N. Uzikov, Izv. Akad. Nauk Kaz. SSR Ser. Fiz.-Mat. No. 2, 15 (1980).
[92]G. Landaud, A. Devaux, P. Delpierre *et al.*, Phys. Rev. C **18**, 1776 (1978).
[93]V. I. Markov and M. A. Zhusupov, in: Prikladnaya i teoreticheskaya fizika (Applied and Theoretical Physics), Kazakh State University, Alma-Ata (1972), p. 84.
[94]J. Erö, Z. Fodor, P. Koncz *et al.*, Nucl. Phys. **A372**, 317 (1980).
[95]L. Vegh and J. Erö, J. Phys. G **5**, 1227 (1979).
[96]M. A. Zhusupov, O. Imambekov, and Yu. N. Uzikov, Izv. Akad. Nauk SSSR Ser. Fiz. **50**, 178 (1986).
[97]L. A. Kondratyuk and L. V. Shevchenko, Yad. Fiz. **29**, 792 (1979) [Sov. J. Nucl. Phys. **29**, 408 (1979)].
[98]G. A. Doskeev, M. A. Zhusupov, and V. I. Markov, Izv. Akad. Nauk SSSR Ser. Fiz. **40**, 742 (1976).
[99]V. S. Borisov, G. K. Bysheva, L. L. Gol'din *et al.*, Pis'ma Zh. Eksp. Teor. Fiz. **9**, 667 (1969) [JETP Lett. **9**, 413 (1969)].
[100]V. I. Kukulin, V. M. Krasnopol'sky, V. T. Voronchev, and P. B. Sazonov, Nucl. Phys. **A417**, 128 (1984).

Translated by Julian B. Barbour